UNIVERSITY OF CALGARY

Comparison of Human and Prosthetic Forefoot Stiffness

by

Mark A. Oleson

A THESIS

SUBMITTED TO THE FACULTY OF GRADUATE STUDIES

IN PARTIAL FULFILMENT OF THE REQUIREMENTS FOR THE

DEGREE OF MASTER OF SCIENCE

DEPARTMENT OF MECHANICAL ENGINEERING

CALGARY, ALBERTA

APRIL, 2000

0-612-49680-5

Abstract

The purpose of this study was to quantify human metatarsophalangeal joint stiffness and compare it to an existing artificial foot which is a candidate for the foot in a shoe testing robot. The study was conducted by examining the forefoot flexion produced by external moments about a Z axis, defined by the horizontal line segment between the 1^{st} and 5^{th} metatarsal heads, a vertical Y axis, and an X axis normal to each.

It was found that for the 6 human subjects tested, the largest stiffness coefficient was about the Z axis with a mean stiffness of 1.1 Nm/deg and a standard deviation of 0.1. An MTS machine was used to measure shoe stiffness, which was then compared with the stiffness of the human foot measured previously using a force plate and motion control cameras. It was found that the stiffness of the shoe about the Z axis was relatively small in comparison to the human foot stiffness. These results showed that shoe stiffness does not dominate that of the foot about the Z axis and that foot stiffness must be incorporated into the artificial foot.

The artificial foot chosen was the Seattle Foot by Seattle Limb Systems Inc. The stiffness of the Seattle Foot was similarly determined by the MTS machine and was compared with the stiffness of the human MP joint. The stiffness of the prosthetic about the Z axis was found to be 37% of the average human stiffness. It was also found that while a human joint rotates about a point, this particular prosthetic foot bends as a beam throughout the forefoot. Thus, a modification to the foot was proposed in which stiff plates would prevent bending along a selected portion of the forefoot, thus increasing the net stiffness of the forefoot. The required dimensions of the plates were calculated based on a theoretical model, and upon testing the stiffness of the modified foot experimentally, it was found that the stiffness had increased to 94% of the desired stiffness, which was within half a standard deviation.

Acknowledgements

Over the past 2 years I have had the pleasure of working with many talented individuals who assisted me in completing this research. I would first like to extend my deepest gratitude to my supervisor, Dr. Peter Goldsmith, for his support, guidance and for always leaving his door open. I would also like to thank Dr. Darren Stefanyshyn for his advice, remarks and especially for pointing me in the right direction throughout various stages of the program.

I wish to thank Dr. Benno Nigg for the conception of the footwear testing robot, for allowing me to participate in the design process and especially for inviting me to the various congresses and seminars which proved to be invaluable in the research.

I acknowledge all the help and input from Trish Balchambers, Dr. Berthold Krabbe, Adidas, Clynch Prosthetics, Seattle Limb Systems, Keith Chrystall, Dr. Simon Monckton, Anne Strock and Dr. H.S. Gill. I would also like to express my gratitude for the input from the robotics group in mechanical engineering for our weekly meetings.

I would like to thank Perry Lang for co-designing and building the testing fixtures and Dean Stanton for the photographs and scanning. Finally I thank my friends James Best, for his support (buying the groceries), Garth Smith for the constructive reinforcement (evening workouts) and especially Michael Dowhopoluk for his friendship (and lending me the money to pay for my tuition).

For my Parents, Marjorie and Brian, without whom I never would have completed... Thank-you.

Contents

Abstract ii

Acknowledgements iii

List of Figures viii

List of Tables xi

1 Introduction 1

1.1 Background ... 1

1.2 Contributions ... 4

1.3 Organization of the Thesis ... 5

1.4 Review of Literature ... 6

2 Anatomical Definitions and Modeling Assumptions 12

2.1 Definitions ... 12

2.2 Anatomy and Foot Modeling ... 16

3 Human Experiment of the MP Joint Stiffness 20

3.1 Introduction ... 20

3.2 Methodology ... 21

3.2.1 Subjects ... 21

3.2.2 Setup ... 21

3.2.3 Data Acquisition ... 22

3.2.4 Data Processing ... 24

3.2.5 Data Analysis ... 24

3.3 Results ... 28

3.3.1 Z Axis ... 28

3.3.2 Y Axis ... 31

3.3.3 X Axis.....32
3.4 Discussion and Stiffness Analysis..... 36
3.4.1 Stiffness about the Z Axis..... 36
3.4.2 Stiffness about the Y Axis..... 39
3.4.3 Stiffness about the X Axis..... 41
3.5 Discussion on Repeatibility.....42
3.6 Summary.....47

4 Shoe Stiffness Experiment 49
4.1 Overview.....49
4.2 Methodology.....50
4.2.1 Assumptions..... 50
4.2.2 Shoe Samples..... 51
4.2.3 Setup..... 52
4.2.4 Procedure..... 56
4.3 Results and Discussion..... 58
4.3.1 Stiffness about the Z Axis..... 58
4.3.2 Stiffness about the X Axis..... 60
4.3.3 Stiffness about the Y Axis..... 62
4.4 Summary.....63

5 Prosthetic Foot Stiffness 64
5.1 Introduction.....64
5.2 Methodology.....65
5.2.1 The Prosthetic Used..... 65
5.2.2 Assumptions..... 66
5.2.3 Setup..... 66
5.2.4 Data Analysis.....69
5.3 Results.....69
5.3.1 Z Axis..... 70

5.3.2 X and Y Axis 70
5.4 Discussion 72
5.5 Summary 74

6 Model For Prosthetic Modification **76**
6.1 Problem and Modification 76
6.2 The Stiffened Length 78

7 Modified Prosthetic Experiment **83**
7.1 Introduction 83
7.1.1 The Modification 83
7.1.2 Methodology 85
7.2 Results and Discussion 85
7.3 Conclusion 87

8 Summary and Conclusion **88**

List of Figures

2.1 Directional Terms........ 13

2.2 Movements of the Foot........ 15

2.3 Anatomy of the Foot........ 16

2.4 Transverse and Oblique Axis........ 18

2.5 Axis Orientation of Foot Segment Coordinate System........ 18

3.1 Marker Location........ 22

3.2 Stages of Gait........ 26

3.3a Z Force (men)........ 30

3.3b Z Force (women)........ 30

3.4a Z Moment (men)........ 30

3.4b Z Moment (women)........ 30

3.5a Z Angle (men)........ 30

3.5b Z Angle (women)........ 30

3.6a Y Force (men)........ 32

3.6b Y Force (women)........ 32

3.7a Y Moment (men)........ 32

3.7b Y Moment (women)........ 32

3.8a Y Angle (men)........ 32

3.8b Y Angle (women)........ 32

3.9a X Force (men)........ 33

3.9b X Force (women)........ 33

3.10 Inversion of the Forefoot........ 34

3.11a X Moment (men)........ 34

3.11b X Moment (women)........ 34

3.12a X Angle (men)........ 35

3.12b X Angle (women)........ 35

3.13a Moments vs. Dorsiflexion (men)........ 37

3.13b Moments vs. Dorsiflexion (women)........ 37

3.14a Stiffness vs. Dorsiflexion (men)........ 38

3.14b Stiffness vs. Dorsiflexion (women)........ 38
3.15a Moments vs. Abduction (men)........ 40
3.15b Moments vs. Abduction (women)........ 40
3.16a Stiffness vs. Abduction (men)........ 40
3.16b Stiffness vs. Abduction (women)........ 40
3.17a Moments vs. Inversion (men)........ 41
3.17b Moments vs. Inversion (women)........ 41
3.18a Stiffness vs. Inversion (men)........ 41
3.18b Stiffness vs. Inversion (women)........ 41
3.19 Non-Normalized, Intra Subject (1) Moment Data........ 43
3.20 Effects of Rearfoot Loading on the Z Axis........ 45
3.21 Moment Caused by Sesamoid behind the Z Axis........ 45
3.22 Effects of Rearfoot Loading on the X Axis........ 46
4.1 Tension-Compression through a Bending Beam or Surface........ 51
4.2 Shoe and Lasts (Z-Axis)........ 53
4.3a Fixture for Z Axis........ 54
4.3b Fixture for Z Axis........ 54
4.3c Fixture for X Axis........ 55
4.3d Fixture for Y Axis........ 55
4.4 True Angle, True Force and the Resultant Moment........ 57
4.5 Z Axis – Shoe Stiffness versus Angle........ 59
4.6 X Axis – Shoe Stiffness versus Angle........ 61
4.7 Y Axis – Shoe Stiffness versus Angle........ 63
5.1 Lifecast Model........ 65
5.2 Foot Fixture Z Axis........ 67
5.3 Z Axis and Fixture Setup........ 68
5.4 Prosthetic Foot........ 68
5.5 Prosthetic Stiffness as a Function of Changing Angle (Z Axis)........ 70
5.6 Prosthetic Stiffness as a Function of Changing Angle (X Axis)........ 71
5.7 Prosthetic Stiffness as a Function of Changing Angle (Y Axis)........ 71
5.8 Prosthetic / Human Joint Stiffness........ 72

6.1 Rotation vs. Bending........ 76

6.2 Beam Bending and Stiffening........ 77

6.3 Deformation of an Element........ 78

6.4 Point Load........ 78

6.5 Applied Moment........ 79

6.6 Point Force Applied to Unmodified Prosthetic Foot........ 79

6.7 Free Body Diagram of Beam with Rigid Attachment........ 80

6.8 The Effects of Changing Moment of Inertia on x_p........ 82

7.1 Rigidity Attachment........ 84

7.2 Foot and Modification........ 85

7.3 Modified Prosthetic Stiffness and Target Stiffness........ 86

List of Tables

2.1 Directional Terms.. 12

3.1 Subjects.. 21

3.2 Intra Subject Standard Deviations.. 42

3.3 Inter Subject Standard Deviations.. 44

4.1 Shoe Information.. 52

1. INTRODUCTION

1.1 Background

The dynamic responses of running shoes have become a recent area of intense focus and investment (Morlock M., 1989). Approximately 15% of all sports injuries involve ankle sprains (Wright I., 1998), which has encouraged sport shoe manufacturers to investigate the relationship between sport shoe design and ankle instability. One objective of a sport shoe is to maintain an effective range of pronation and supination, defined in Chapter 2. These motions are required during the heel strike phase of the gait cycle in order to cushion the impact force but should be limited in order to minimize strains on the ligaments (Nigg, 1986). Comfort, durability, and injury prevention requirements, have led to improvements regarding the manner in which these products are tested. Due to the highly specialized and extensive tests required to perform sport shoe evaluation based on biomechanical testing, the results are often presented long after the product has been released into the market.

Currently, most studies on running shoes are performed using simulation software or actual test subjects. Unfortunately, mathematically based shoe simulations cannot predict all the responsive dynamic forces in the shoe and data from human test subjects is difficult to process and is non-standardized due to each individual's distinct gait cycle. This lack of standardization increases the difficulty in comparing one shoe with another. In addition, the intra-subject data is also not always repeatable which affect data's reliability. Thus, standardization of the testing methods would be preferable so that one shoe may be compared with another. It would be desirable to have a repeatable subject that could also function as a statistical representation of all subjects.

Since such a subject does not exist, using a robotic sport shoe testing system that mechanically simulates human movement and control would be an original approach to solving these problems. This novel approach of introducing robots was proposed recently by a group of researchers at the University of Calgary in collaboration with the Alberta Research Council and Adidas. This robot will be the first attempt to simulate the motion of the human leg based on simulated trajectories and will iteratively modify its gait based on the reaction forces retrieved from the force sensor in the robot's ankle. This force data will serve as a new input variable to the simulation which will then alter the following position trajectory. Robots have, in the past, been used to perform human tasks, but did not move or conduct these tasks in a human manner. In this case, the robot will functionally walk as a human, and will modify its gait depending on the responsive forces. The robot is to be based on a Stuart Platform or hexapod. Instead of designing a functional ankle, a foot will be rigidly suspended from a platform, and by using inverse kinematics, the ground, controlled by the hexapod, will move up to the foot, thus replicating the same impact and pushoff dynamics. Bejune et al. (1994) had also developed a prototype footwear testing machine which attempted to simulate a human gait cycle with only 2 degrees of freedom. Due to its basic construction and limited control system, the robot was not able to replicate the human gait successfully.

This new robot will be controlled by a novel control approach called Quasi-static Simulation Control (P.Goldsmith 1999) and will improve its accuracy using a test procedure called the Dynamic Correction Method (P.Goldsmith 1999). Along with the 6 degrees of freedom made available by the robot's construction, this robot is the first to replicate and modify any human's gait while providing force feedback to measure the effects on the ankle joint.

The proposed robot will perform activities to simulate human athletics such as running and side cutting. In doing so, it allows for an analysis of the dynamic responses of the shoe and ankle. Control of the robot will mechanically replicate human ankle and leg during running and side cutting motions. However, the foot will be completely passive and must emulate the compliance of a real foot throughout the gait cycle.

One parameter for such a design is the compliance and stiffness of the forefoot with respect to the rearfoot. Stefanyshyn and Nigg (1997) have determined how the dynamic angular stiffness of the ankle is influenced by different activities and have quantified the relative contribution of the metatarsophalangeal joint to the total mechanical energy in running and sprinting, but had not extended the notion of stiffness to the forefoot joints. Quantifying stiffness would be a practical way of comparing a human foot with a model foot which would function as the end effector of the robot. Very few studies have analyzed forefoot-rearfoot motion, and it seems that none have quantitatively measured the stiffness about the metatarsophalangeal (MP) joints. In fact, one of the most common biomechanical models of the foot is a single rigid body allowing only a progression angle and net dorsi-plantar flexion to be measured (Carson et al, 1998). However, the foot is a multi-segmented model in which the forefoot acts as a rigid lever independently of the rearfoot segment throughout the push off stage of the gait cycle (Donatelli, 1990).

It is proposed that the foot be modeled as a passive object with 2 rigid members, the forefoot and rearfoot. These rigid segments are modeled such that they are separated by a compliant metatarsophalangeal joint, which has a specific stiffness coefficient. Of course, in reality these metatarsophalangeal joints do not act at one joint along the same axis of rotation, but since the shoe bends primarily along 1 single axis, this study has simplified the mechanical model to a single axis connecting the 1st and 5th metatarsal heads.

One of the needs of the robotics project is to determine an appropriate model of the human foot which may be used with the robot as a realistic interface between the shoe and the robot. Furthermore, based on the needs of this robotics project, the available equipment and the current literature, the aim of this study was:

- To determine experimentally the stiffness coefficients of the human metatarsal joint along 3 axes during running.
- To quantify the stiffness of a prosthetic foot so that it may be used as the foot of the robotic unit; and to conduct a comparison between the prosthetic and the real foot.
- To determine and test a simple modification to the prosthetic such that its stiffness more closely resemble that of a human foot.

1.2 Contributions

The contributions of this thesis may be summarized as followed:

- Quantified the stiffness coefficient about the metatarsophalangeal joint during the pushoff stage of a running gait.
- Determined the stiffness of running shoes about the same axes defined for the human test subjects.
- Evidence that the prosthetic stiffness is approximately 37% of the human MP stiffness.
- Modification of the prosthetic stiffness to within 6% of the human stiffness.

1.3 Organization of the Thesis

Chapter 2 will provide the reader with basic definitions and the anatomic and functional framework for the mechanical model. This chapter will be essential for a complete understanding of the experiments in the sections that follow. Chapter 3 determines and discusses the stiffness coefficients about the MP joints in the human foot. This section will provide the template of the dynamic stiffness that the artificial foot will attempt to replicate. Chapter 4 discusses shoe testing, which was reported in order to determine the stiffness about the same axial orientations in the human foot. This experiment will indicate whether or not the foot stiffness about a given axis is large or small compared to the shoe stiffness. It is conjectured that if the stiffness of the shoe dominates that of the human foot, then the behavior of the foot-shoe combination will be dictated primarily by the shoe, and not the foot. This may simplify the performance requirements in the artificial foot for a given axis. The prosthetic foot was tested in Chapter 5, and compared to the human mechanical model. Chapter 6 provides a basic theoretical justification for a proposed simple modification on the prosthetic foot, and Chapter 7 will present the experimental testing of the prosthetic and its modification along with a comparison to determine if it has been an improvement to the design. A brief summary of the experiments and the findings, with respect to the objectives, is provided in Chapter 8.

1.4 Review of Literature

In this section, a brief outline of various biomechanical research sources is cited. The literature presented in this section comprises the fundamental ideas that were required for the research, which will be presented in future chapters.

Modeling joints in terms of stiffness by no means a new concept. Recently, Stefanyshyn and Nigg (1998) modeled the ankle joint using a torsional stiffness coefficient. This type of stiffness was termed "quasi-stiffness" by Latash et al. (1993) since it is defined as being the moment divided by the angular displacement. Stefanyshyn and Nigg determined the relationship between the ankle joint moment and the respective angle. In quantifying values they hypothesized that the ankle could be approximated by a linear stiffness, and that this stiffness would be dependent upon the activity. In the Stefanyshyn and Nigg study, the results were compared with the single linear stiffness data obtained from a previous study (Davis, Deluca, 1995), which quantified ankle stiffness for 50 percent of the stance phase during walking.

Historically, moment-joint relationships have been researched (Hunter and Kearney, 1982) using isokinetic devices with exceptions including Davis et al, and Stefanyshyn and Nigg. However, very little research has been focused on applying these 'dynamic stiffness concepts' to the metatarsophalangeal joint, which is responsible for the phalangeal bending during pushoff. Research by Dozzi et al. (1989) observed the metatarsophalangeal power required during jumping in ballet and found that the muscles near the metatarsophalangeal joints do provide a great deal of power about the joint with respect to the MP cross-sectional area. It is conjectured that for this reason, the metatarsal bones are often injured. This was further shown to affect the distal ends of the 2nd and 3rd metatarsal bones when Hong and Gu (1997) calculated the dynamic shear stress applied while walking on flat ground.

Due to its superior size and strength, some early research had focused solely on the 1st metatarsophalangeal joint and the motion it provides to the hallux. Joseph, J. (1954) determined that the allowable motion about this joint was extremely individualistic, but in all cases, was much freer in dorsiflexion than in plantar flexion. The mean values of maximum dorsiflexion were found to be 52 degrees while the neutral position was initially at 15.8 degrees dorsiflexion. This motion would have significant applications in the 'pushoff' phase of a gait cycle. However, it may be conjectured that since the joint is flexible in dorsiflexion, it may not have extremely stiff characteristics. However, Joseph's research further shows that the range of the metatarsophalangeal joint in dorsiflexion is significantly greater than the range of the interphalangeal joints. This smaller range of motion about the interphalangeal joints provides the basis for modeling the portion of the foot distal to the MP joint as one rigid body.

Studies by Mann and Hagy (1979) showed that the toes' principle function was that of stabilizing the longitudinal arch and to maintain floor contact during walking. In running, the intrinsic muscles of the toes were much more active and assist forward propulsion of the body. All of these motions were naturally about the metatarsophalangeal joint. Similar research by Bojsen-Moller and Lamoreux (1979) focussed on the significance of dorsiflexion of the toes in walking. This research shows not only the anatomical range and significance in dorsiflexion, but also demonstrates the motion as a function of gait. Bojsen-Moller and Lamoureux show that, unlike the fingers, the significant range of motion lies in dorsiflexion about the metatarsophalangeal joint. This range about the metatarsophalangeal joint ranged from the maximum dorsiflexed position at pushoff, which was 58 degrees, to a minimum value at heel strike, which was 25 degrees of dorsiflexion. This dorsiflexion is described as being essential for the function of the entire foot as it supports, and stabilizes the ball of the foot to any tangential forces to which it may be exposed. This research however differs from Mann and Hagy in that it is inferred that the motion of the toes are more forced into their positions due to the weight of the body.

Further research by Hetherington, Johnson and Albritton (1990), concentrated on redefining the amount of dorsiflexion required during gait. This paper hypothesized that a minimum value of dorsiflexion must be obtained for the hallux in order for appropriate propulsion to take place. The article also points out the differences in previous literature regarding the range of dorsiflexion about the metatarsophalangeal joint. This research also provided experiments which showed a functional dorsiflexion maximum of 50.5 degrees, which is mentioned as mostly resembling the value obtained by Bojsen-Moller and Lamoureux. Fulford et al. (1989) were some of the first individuals to include inversion and eversion within their study of dorsiflexion about the metatarsophalangeal joint. Their research focussed primarily on the dynamic dorsiflexion of the hallux and supination of the forefoot of children with neurological disorders.

Recently, studies by Davies (1999) and Lee (1997) focused on additional motions of the forefoot with respect to the rearfoot other than dorsiflexion. Lee's research showed adduction and abduction of the forefoot with respect to the rearfoot. This study showed an average of 9.3 degrees of relative forefoot abduction with respect to the rearfoot during running.

Researchers such as Chan and Rudins (1994) have contributed significantly by designing models to describe the biomechanics of the foot during various running and walking gaits. These models are relatively extensive in that Chan and Rudins described foot motion about all the rotating axes of the heel and proceeded to include the metatarsophalangeal joint.

In addition to research on the motion and anatomical response of the forefoot, many other studies have included the forefoot in their models of the foot and leg. The current modeling approaches seem either tailored for simulation and indirect force determination (M.Morlock, 1990) or into less elaborate, more functional models. Stokes et al. (1979) proposed one of the first MP inclusive models which was used to estimate the forces acting on the metatarsophalangeal joints during normal walking. This model was used in quasi-static evaluation testing and was two-dimensional. Stokes' model was later improved upon by Salathe and Arangio (1986), who determined the theoretical forces acting upon the metatarsal heads. This theoretical model included 4 rigid bodies and was used in calculations for various activities. They had concluded that pronation and supination greatly affect the force distribution on the metatarsal heads. More complex theoretical models of the foot were later designed to include the metatarsophalangeal joints. Morlock (1989) had increased the number of rigid bodies in his MP inclusive model to six and found that there was no benefit in increasing the degrees of freedom past six. Scott and Winters (1993) had also created a foot model involving 8 rigid bodies, but had limited the degrees of freedom between 2 connecting bodies to one. Further models were created and elaborated upon (I.Wright, 1998), but may have been overly complex for dynamic, invivo studies and are more applicable to indeterminate, theoretical simulation programs.

Since this research is concerned with the metatarsophalangeal joint, the model proposed in this research will resemble the models suggested by Stefanyshyn and Nigg (1997). The purpose of their research was to quantify the amount of mechanical energy used by the metatarsophalangeal joint during running and sprinting. This was the first study to research the amount of energy supplied by the metatarsophalangeal joint since a study involving only one subject by Elftman (1940). This research had determined that the MP joint was a large energy absorber with value ranging from 20.9 J in running to 47.8J in sprinting. This model is extremely important in that it defines the distal portion of the MP joint and onwards as 1 rigid body, and defines the rest of the foot as a separate body. This framework will allow for relatively simple calculations of the moments acting upon the MP joints. As a result of Stefanyshyn and Nigg's research, an opportunity to apply the stiffness concepts they had applied previously to the ankle may also be subjected to the metatarsophalangeal joint of which they had calculated energy contribution. This concept of quantifying stiffness will simplify the comparison between human and mechanical joints.

With so much research focussing on the human foot, it would seem as though there should be a reasonable amount of literature focussing on mechanical foot models or prosthetic frameworks. This is not entirely true due to the design motivation behind prosthetic research. The goal of the prosthetic is not to replicate the responsiveness of a human foot, but to enhance the individuals gait. For this reason, most evaluation techniques of prosthetics are based not based on comparative studies in relation to human foot performance, but more guided towards mechanical efficiency and gait evaluation of amputees. These evaluation techniques will be discussed further in Chapter 5.

2 Anatomical Definitions and Modeling Assumptions

This chapter provides the definitions and the framework for the modeling of the experiments presented in the following chapters. In Section 2.1 of this chapter, a brief review of the anatomy and the pertinent definitions will be presented. This terminology is crucial for understanding the following chapters. This will be followed by Section 2.2, which will provide a brief geometric explanation of the foot model and the reasons why it was chosen.

2.1 Definitions

The terms defined in this section are used throughout due to their precise meaning and will reduce the need to use additional descriptive words. Table 2.1 and Figure 2.1 exhibit the directional terms, which will be used to define joint motions and anatomical members.

Lateral	Farther from the midline of the body/structure
Medial	Nearer to the midline of a body/structure
Proximal	Nearer to the point of origin
Distal	Farther from the point of origin
Anterior	Nearer to the front of the body/structure
Posterior	Nearer to the back of the body/structure

Table 2.1: Directional Terms

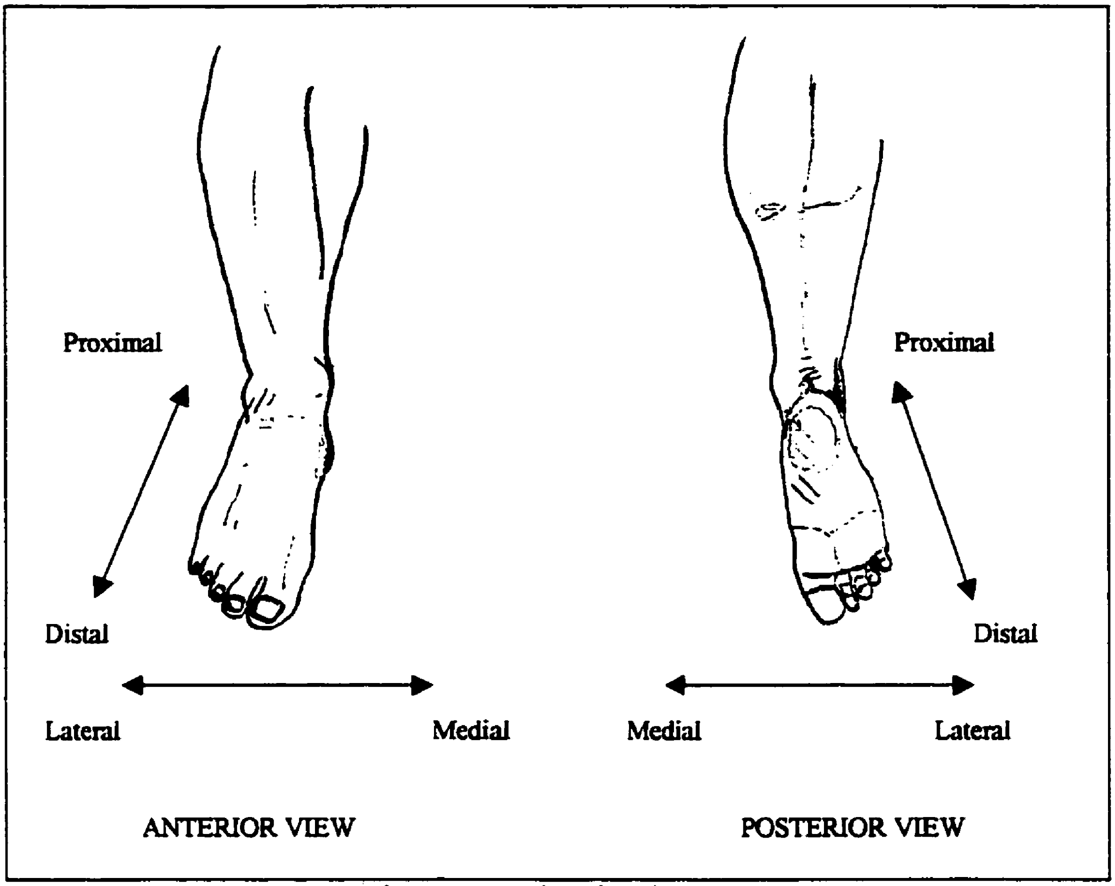

Figure 2.1: Directional Terms

In defining the joint motions, there must first be an understanding of the planes in which the motion occurs. The primary planes of motion in the foot and ankle are the frontal, sagittal and transverse planes.

The sagittal plane passes through the body in an anterior-posterior orientation while being perpendicular to the ground, thus splitting the body into left and right parts. The frontal plane separates the body into anterior and posterior parts while being perpendicular to the ground and normal to the sagittal plane. The transverse plane passes through the body horizontally and is thus parallel to the ground (Morlock, 1989).

The X axis is defined by the line comprised of the intersection of the sagittal and transverse planes. The Y and Z axes are similarly defined by the lines obtained through the frontal-sagittal and the frontal-transverse plane intersections respectively.

One of the purposes of this research is to analyze joint motion, which is assumed to be a purely rotational motion and whose movements travel in an arc about a reference point or joint center (Donatelli, 1990). The three principle rotational movement components of the foot may be defined as being dorsiflexion-plantarflexion, inversion-eversion, and adduction-abduction. In addition, motions about all three planes may be termed 'supination' or 'pronation'. These terms will be further discussed as being combinations of the three primary motions.

As shown in Figure 2.2, eversion-inversion, adduction-abduction, and dorsiflexion-plantarflexion, are motions which occur in the frontal, transverse, and sagittal planes respectively. These motions, being purely rotational, occur about axes parallel to the X, Y or Z axes respectively and passing through the joint center. These axes will be given specific orientations with respect to the biology of the foot in Section 2.2.

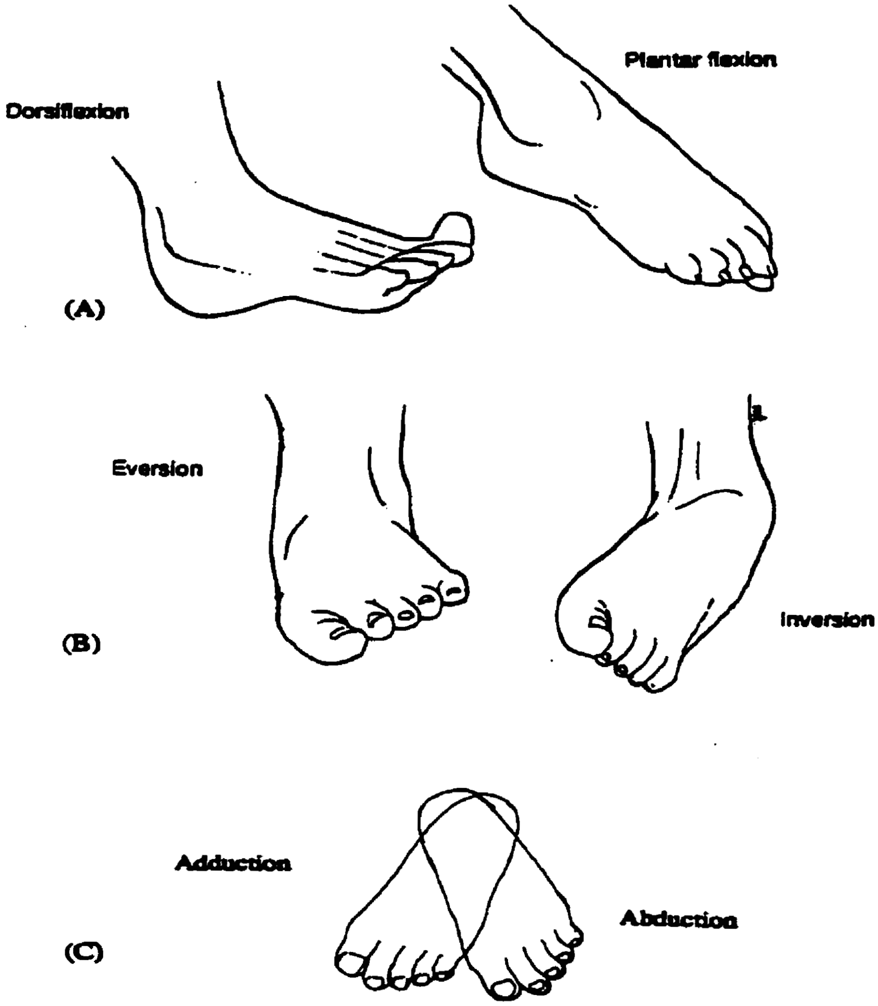

Figure 2.2: Movements of the foot (Morlock, 1989)

Supination and pronation refer to motions which result in deflection angles about each of the body planes (Root, 1977). Pronation occurs when one member everts, dorsiflexes and abducts with respect to another member of the body. Inversion, adduction and plantarflexion of a jointed member with respect to another member is called supination.

2.2 Anatomy and Foot Modeling

The human foot consists of 11 extrinsic muscles, 26 bones and over 100 ligaments and is often divided into 3 regions. Hawes et al define the hindfoot as being composed of the calcaneus and the talus bones, the midfoot composed of the navicular, the cuboid and the 3 cuneiform bones, and the forefoot as being the remaining front portion composed of the metatarsals and the phalanges (Hawes et al, 1997). Between the metatarsals and the phalanges sits a series of joints called the metatarsophalangeal (MP) joints, which allow the phalanges to rotate about the metatarsal heads. Since this research examines solely the stiffness of these joints, it is useful to redefine the forefoot, shown in Figure 2.3, as being only the phalanges, while the rest of the foot will be termed the rearfoot. One limitation of this research is that, despite the number of bones and joints in each division, both the fore and rear foot will be assumed to be rigid. This research assumes that the metatarsophalangeal joints allow 3 degrees of freedom between these two members, all of which are rotational. B.Nigg (1994) defines such joints as spherical, and thus assumes that there is no translational motion between the members.

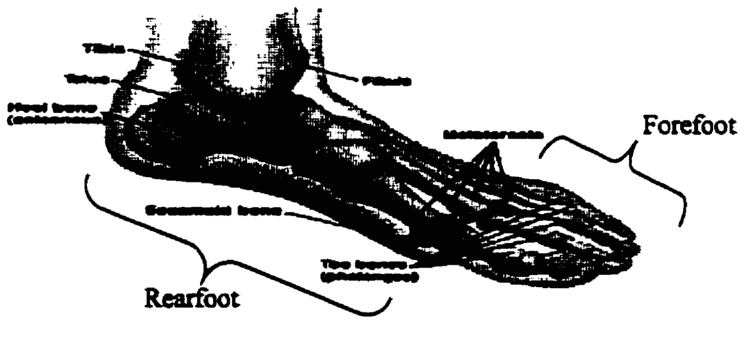

Figure 2.3: The Anatomy of the Foot (orthoknow.com/anatomyfoot.htm)

The rearfoot has one distinct protrusion located just behind the first metatarsophalangeal joint and medial to the joint center. This protrusion is due to the sesamoid bone, which is the attachment site for many soft tissues and house the flexor mechanisms like the flexor hallucis longus tendon. The important characteristic about the sesamoid is that it is located very close to the MP joint and it absorbs most of the vertical pressures during push-off.

The metatarsals and phalanges will be referred to as the first through to the fifth depending on their order with respect to their medial position. For example, the metatarsal of the hallux, or big toe, will be referred to as the first metatarsal, while the fifth metatarsal refers to the small toe. These metatarsal heads do not form a straight axial line but instead form two principle axes upon which the rotational motions occur. The transverse axis runs from the first to the fifth metatarsal head and is described by Bojsen-Moller as being used for high gear push-off. The oblique axis runs from the second to the fifth metatarsal head and is a lower gear axis (Bojsen-Moller, 1979). However, since the forefoot has been defined as a single rigid body, there must be one axis for all the MP joints. For simplicity, this axis was defined as the line connecting the first and fifth metatarsal heads, shown in Figure 2.4. In addition, this axis will be located on the frontal and transverse plane and will be referred to as the Z axis. This axis runs through the foot in order to approximate the joint centers of the MP joints. The implications in defining the Z axis in such a way is a limitation in the research in that the individual MP joints are ignored and only the rotation of the entire forefoot will be analyzed. This will also affect the assumption that the forefoot is a rigid body. Since there is relative rotation from one MP joint to another, the markers placed on the forefoot, used to define a rigid body, will move relative to each other which affects the rigid body assumption. The less rigid our forefoot is, the less accurate will be the relative angle data between the forefoot and the rearfoot retrieved from the motion analysis cameras. The angles were found by defining 2 rigid bodies, using markers, and calculating the relative rotation between the two. When these markers move, the rigid bodies in our physical model are altered.

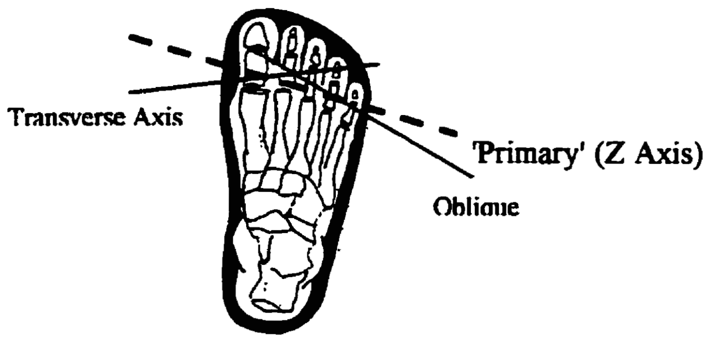

Figure 2.4: Transverse and Oblique Axis (Bojsen-Moller 1979)

The Y axis is oriented in a positive vertical direction when the foot is in neutral stance and intersects the midpoint of the segment joining first and fifth metatarsal heads. Lastly, the X axis is simply the normal of the Z and Y axes and is anteriorly positive as shown in Figure 2.5. Figure 2.5 also shows that the axes form a left hand coordinate system chosen to conform with the experimental orientation and the software used.

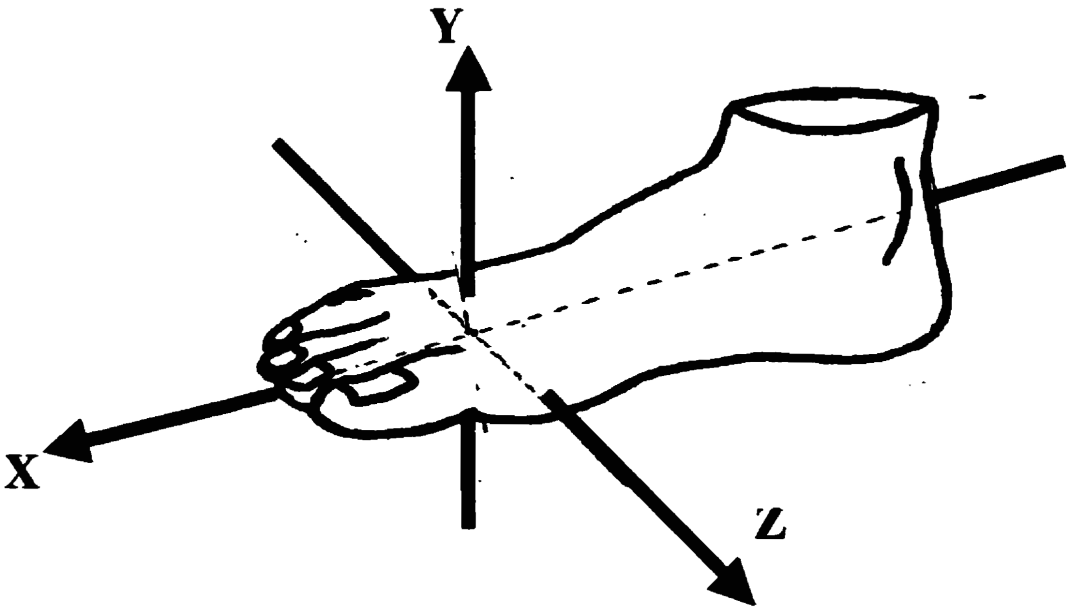

Figure 2.5: Axis Orientation of foot segment coordinate system

Throughout this experiment, a passive foot is assumed so that the human foot can be compared with the artificial foot. In other words, since the artificial foot has no internal drives or power source, it can only react to external forces. An assumption that the forefoot-rearfoot moments are passive reactions so that a stiffness coefficient may be defined about these axial joints. This implies that no muscular activity is present to increase the joints' rigidity, which is not the case. However, this assumption is crucial in defining pure moment reactions since the artificial foot will not have any rigidity control as its human counterpart does.

3 Human Experiment of the MP Joint Stiffness:

3.1 INTRODUCTION

In the analysis of the gait cycle, the foot is often defined as a rigid body. However, when the goal is to analyze the 'push-off' phase of running, this model becomes too oversimplified (Morlock, 1990). The human foot, being an extremely complex structure, has 33 complex joints, which allow for intentional and responsive motion, (Toratora, 1996). The metatarsophalangeal joints, (or MP joints) define a border in the forefoot between the toes and the remainder of the foot, and are primary agents in the push-off phase of running (Mann & Hagy, 1979). This chapter will determine the relative stiffness coefficient about the metatarsophalangeal joint using human test subjects. These stiffness coefficients about the MP joint will be used as the model which will be compared with a prosthetic foot's mechanical behavior during push-off. The prosthetic used is the Seattle Foot (model:SFH110) made by Seattle Limb Systems.

Section 3.2 of this chapter will describe the methodology of the experiment in terms of the assumptions, the subjects, the data acquisition procedure and the tools used in the data analysis procedure. This will be followed by Section 3.3, which will provide the overall results of these tests regarding the moments, forces and angles obtained. Section 3.4 will analyze the results from each axis in depth, describing the motion and stiffness coefficients obtained and potential problems with the data. Finally, Section 3.5 of this chapter will briefly discuss the errors and repeatability, and Section 3.6 will summarize the findings of this experiment.

3.2 METHODOLOGY

3.2.1 Subjects

In this experiment, 3 subjects of each gender were used based on the standards determined by the Adidas Testcenter. However, 4 were tested so that one may be removed if an extreme outlier were to occur. Two groups of four were made, male and female. All subjects were between the ages of 20 and 35, and had no medical afflictions. In addition, all were moderate to active in their sports activities. Table 3.1 below lists the subjects and any relevant information.

Name	Sex	Height (cm.)	Weight (Kg.)
Subject 1M	Male	183	84
Subject 2M	Male	170	70
Subject 3M	Male	168	74
Subject 4M	Male	179	82
Subject 1F	Female	165	61
Subject 2F	Female	168	64
Subject 3F	Female	172	61
Subject 4F	Female	162	58

Table 3.1: Subjects

3.2.2 Setup

This experiment was performed in the Human Performance Lab at the University of Calgary and was supervised by the staff working under Dr.Nigg and Dr.Stefanyshyn.

First, the subjects were to remove all footwear since the experiment was to analyze the barefoot gait. Reflective ball markers, 1.2 centimeters in diameter, were strategically placed on the right foot so the positions of specific segments may be tracked. Figure 3.2 describes the placements of these markers.

Markers	Location Name
1	Medial Ankle
2	Lateral Ankle
3	Proximal Calcaneus
4	Distal Calcaneus
5	Posterior Calcaneus
6	5th Metatarsal Head
7	2nd Metatarsal Head
8	2nd Phalange
9	1st Metatarsal Head

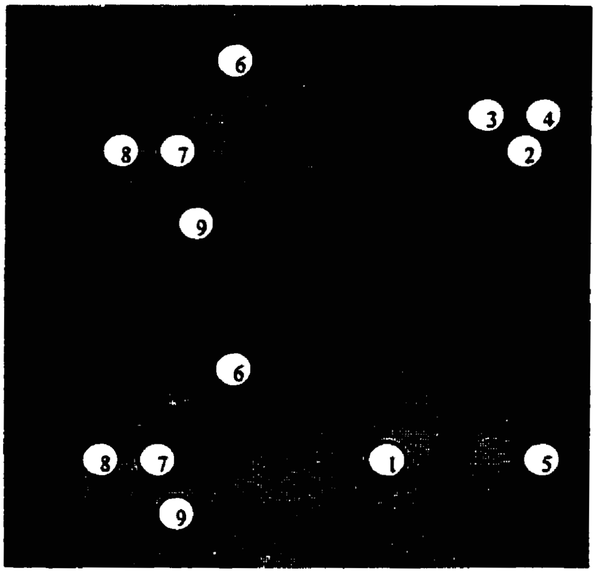

Figure 3.1: Marker Locations

Markers 1 and 2 were chosen to define the joint center of the ankle but were not required for this research. Markers 3, 4, and 5 define the planar surface of the rearfoot. These rearfoot markers will define the motion that occurs in the rearfoot, and will be used to measure the rotation in the forefoot. Markers 6, 8, and 9 define the forefoot, as defined by Lee when determining forefoot ab-adduction (Lee S., 1997). The rotation information is this planar surface with respect to the reference plane defined by the rearfoot markers. Marker 7 was used to define the meeting point of the transverse and the oblique axis, which was not required, but may be used be in future studies.

3.2.3 Data Acquisition

The subject was required to run at 4 meters per second (± .2) and were to land on his/her right foot in the middle of a Kistler force plate, model Z4952c, which sampled the data at

2400 Hz. The force plate has a transducer on each of the four corners, and allows us to determine the forces and moments along all three axes with respect to a force-plate coordinate system (Nigg B., 1995). Before each test, the force plate was reset to zero.

Six high speed Falcon 240 Motion Analysis Video Cameras of Santa Rosa, California, were placed around the field in which the subject was to run across the force plate. The cameras were set to a 240 Hz sampling rate with a 6.0 mm Computar lens and were used to measure the positions of each marker, with respect to a lab coordinate system through its connection to the lab's MIDAS system. The cameras were placed around the force plate and were placed at different heights and various angles so that a minimum of 4 cameras would be able to see any marker at any given time. The cameras are calibrated using known forms with known geometries. With a known geometry the system can orient itself relative to the other cameras and the collection volume. For this, a cube and a moving wand were tracked for a 90 second sampling period at 240Hz. The software, Eva 5.00, is programmed to know the geometry of the wand and the cube used. Tracking of the points was also conducted using EVa Version 5.00. As the subject ran, he/she triggered a motion sensor, which signaled the cameras and the force plate to begin the data collection. This trigger ensured that the force data and the position data began sampling simultaneously.

3.2.4 Data Processing

The running data obtained comprises of position data sampled at 240 Hz with respect to a lab coordinate system, and force data sampled at 2400 Hz with respect to a force plate coordinate system. The tracked data was transformed such that it was with respect to the segment coordinate system defined about the MP joint center. Basic weighted averaging procedures were used with Matlab 5.2 so that the final data was with respect to the segment coordinate system at a sampling rate of 240 Hz.

In order to determine the angles between the segments, cardanangles were used. The first angles measured were about the Z axis followed by the X and Y consecutively. Since the Z axis was the first rotation, it will be called the primary axis. The order upon which these angles were measured had to be repeated since a different order could result in a different angle value.

3.2.5 Data Analysis

Each position data file was tracked individually using Eva Version 5.0. The coordinates of each marker were determined through the Motion Analysis Cameras and MIDAS.

Because the force and position data were sampled at different rates, it was necessary to normalize the sample frequencies. The trials of every subject's force data was sampled at 2400 Hz, and in order for the force data to correspond with the appropriate points from the position data, sampled at 240 Hz, the discrete data points must be normalized to the same temporal scale as the position data. Thus, the points from both force and position were extracted at a frequency of 240 Hz. The frequency of the force data was brought down to 240 Hz simply by using a floating point average over 10 points which also filtered out any high frequencies.

$$f_{240}(i) = \sum_{j=10i-9}^{10i} \frac{f_{2400}(j)}{10} \quad (3.1)$$

where $f_{240}(i)$ = the value of the force in the i^{th} position of the 240 Hz force file,

and $f_{2400}(j)$ =the value of the force in the j^{th} position of the 2400 Hz force file.

A simple floating point average followed by a spline to normalize the data was used. This data was to be used in a calculation to determine the mean force, and thus any small errors caused by noise will be negligible in the final output. The noise frequencies are dealt with by the floating point and spline combination used in order to obtain the lower frequency of 240 Hz used.

The position data was smoothed somewhat in order to aesthetically smooth the slopes connecting the data points. This required a mean percentage to be used for each discrete point *X* using weights of 0.1 for *X-2* and *X+2* points and .2 for values *X-1* and *X+1* points with a value of .4 for *X* itself. These points minimized the noise significantly and by using a spline, we were able to normalize the curve such that each data file would contain n discrete points. Since the objective is to obtain an overall stiffness for the entire gait cycle, this smoothing process of the curve will not affect the results and was done for aesthetics.

In order to analyze the data, the following conditions should be noted. Due to the axis orientation, some of the forces and angles were negative but since the magnitude of the stiffness was to be compared with the stiffness of prosthetics all stiffness coefficients will be positive. Secondly, angles are measured from the neutral position of the foot, and so a negative angle deflection about the Z axis, for instance, is caused by the dorsiflexion of the toes about the MP joint. Since the Z axis of the segment coordinate system is positive in the lateral direction, a negative moment will result in a negative angle increment or dorsiflexion.

The speed of the runner will affect the graphical position of the event peaks, and thus the event peaks are synchronized each other, creating a series of event normalized curves. The event that this experiment is concerned with is the push-off stage of the gait cycle, which is the third stage of Figure 3.2.

1) Heel Strike: Vertical force exceeds 0 newtons

2) Flatfoot: Relative angle about Z with respect to the ankle ~0

3) Push-Off: Negative Moment about Z-Axis

4) Toe-Off: Vertical Force returns to 0 newtons

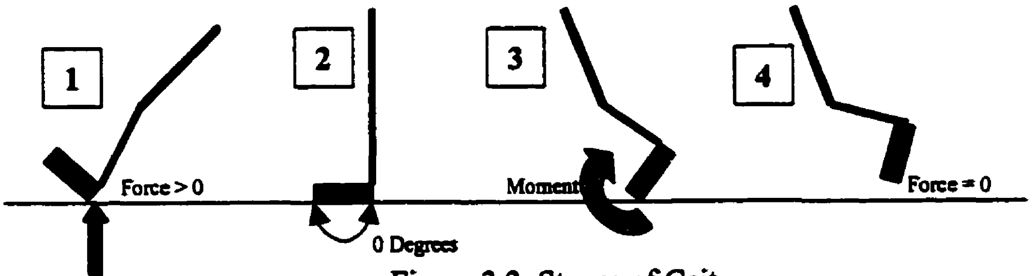

Figure 3.2: Stages of Gait

The methodology described above was applied to 8 subjects, 4 for each gender. Each subject's data is comprised of 10 trials. In addition, each of these subjects has angle and moment data with respect to each axis in the segment coordinate system. Due to the small approximate moment of Inertia value, the Inertia and rotational effects on the moment will be dropped resulting in a moment calculation based on the magnitude of the force multiplied by the distance between the force centroid and the MP axis.

3.3 Results

In the following section, the moment and angle data will be presented for each individual axis. The data presented is about the segment coordinate system, which is defined in Chapter 2, and may be negative in their values. All data provided commences at the initial stages of push off which is defined by the occurrence of a negative moment about the defined MP Z axis, representing 0 percent event-time.

3.3.1 Z-Axis

The Z-Axis is our primary axis of rotation, which is defined by the line extending beyond the segment joining the 1st and 5th metatarsophalangeal joint heads. We first note that the force shown in Figure 3.3 (a & b) is almost perpendicular to the direction in which the subject is running and thus may be one of the factors in determining moments along the X and Y axes. We do note that though the curves do not seem to follow similar trends, but are not synchronized with each other. This force being positive indicates that the force is being exerted laterally just before toe-off. This may be a large indication that supination of the entire foot is greatest at 80 percent of the event time in the push-off stage of the gait cycle.

The moment data obtained about the Z-axis is obtained by the force and position data along with the basic Neutonian moment equation

$$\sum M = F \cdot d + I \cdot \alpha \tag{3.2}$$

However, if the moment of inertia of the forefoot was calculated similarly to that of a cross sectional rectangle, then

$$I = \frac{1}{12} a \cdot b^3, \tag{3.3}$$

where a and b are dimensions of the forefoot. Since these are relatively small, it is assumed that that the effects of the angular acceleration and the moment of inertia are negligible.

The distributed forces about the foot are grouped, and converted to a point force with a point of application determined by the force centroid. The moment about the Z axis will be the largest and is caused by the roll onto the phalanges resulting in dorsiflexion about the MP joints themselves. As shown in Figures 3.4a and 3.4b, the moment is negative for the duration of the push off phase reaching a local maximum, at approximately 50 percent pushoff, before returning to 0. This large negative moment indicates that the moment is applied counterclockwise to the positive Z axis. In examining this moment data in conjunction with the angle data, we note that the moment is positive for the first 5-10 degrees of dorsi-flexion. This is due to the major weight bearing of the sesamoid due to its location behind the MP joint, and its protrusion with respect to the other bones in the vicinity. Thus the rearfoot begins to lift and the phalangeal bones begin to rotate with respect to the rearfoot due to the MP joints' compliance about the metatarsals. Thus, phalangeal dorsiflexion commences before the affecting net moment is applied. The dorsi-flexion continues to a maximum of approximately 39 and 34 degrees for men and women respectively at 90 percent push-off, and finally begins toe off as it returns to a neutral position as shown in Figures 3.5a and 3.5b. In addition, the absolute moment decreases midway through the push-off stage while the angle of flexion continues to increase until the last 10 or 15 percent of the state. This may result in a non-linear relation between the moment and angle.

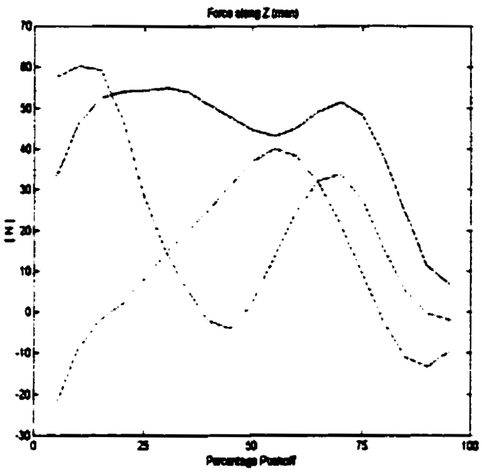

Figure 3.3a: Force on the Z Axis -Men

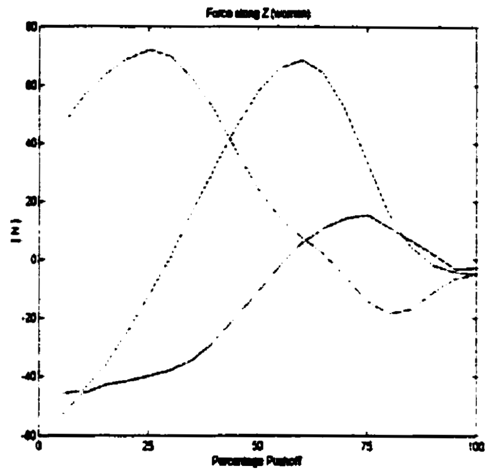

Figure 3.3b: Force on the Z Axis -Women

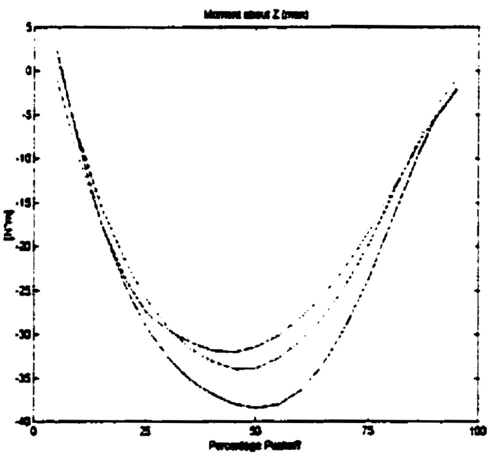

Figure 3.4a: Moment about Z Axis –Men

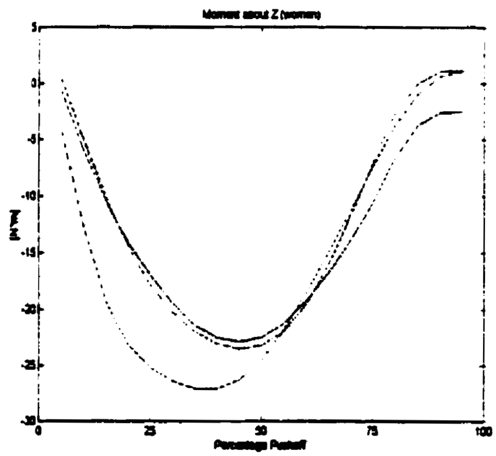

Figure 3.4b: Moment about Z Axis –Women

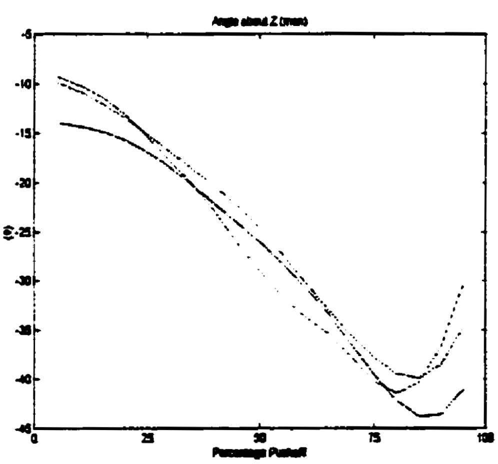

Figure 3.5a: Angle about Z Axis -Men

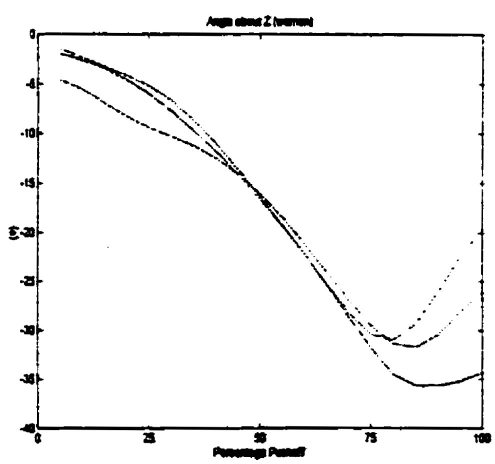

Figure 3.5b: Angle about Z Axis -Women

3.3.2 Y-Axis

The forces corresponding to the Y axis show that the initial stages of push-off demonstrate the greatest amount of force received by the force plate (not including heel strike or any subsequent stages up to push-off). The forces range from 1600 N to 2200 N as shown in Figure 3.6a and 3.6b. These forces are the largest contributors to the moments occurring about the Z axis.

The angles about the Y axis show that the pushoff stage of the gait cycle results in a metatarsal trend towards abduction of the forefoot with respect to the rearfoot. This is due less to the forefoot motion, and more a cause of the movement of the rearfoot and ankle. The abduction about the MP joint shows that supination of the foot seems to be occurring due more to the adduction of the ankle and less due to the MP relative abduction about the Y axis.

In observing the moment about the joint shown in Figures 3.7a and 3.7b, the change from adduction to abduction occurs almost simultaneously with the crossover of the moment from positive to negative. However, the data also shows in Figures 3.8a and 3.8b that the abduction about the axis continues to increase up to 100 percent and 90 percent (men and women respectively). Meanwhile, the moment has reached its maximum value of 4.9 Nm (men), and 3 Nm (women) and had begun to return to zero. This may be a result of surrounding muscular contraction, but will likely cause difficulties in our spring model due to its non-linear behavior. Fortunately, the deflection values are fairly small reaching only a maximum abduction angle of less than 8 and 6 degrees for men and women respectively.

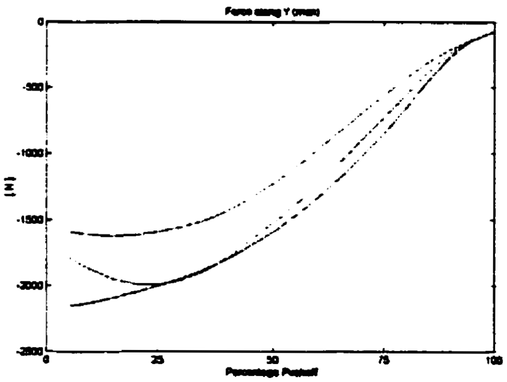

Figure 3.6a: Force Y Axis -Men

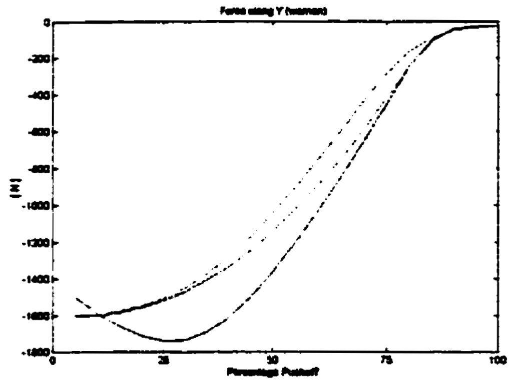

Figure 3.6b:Force Y Axis -Women

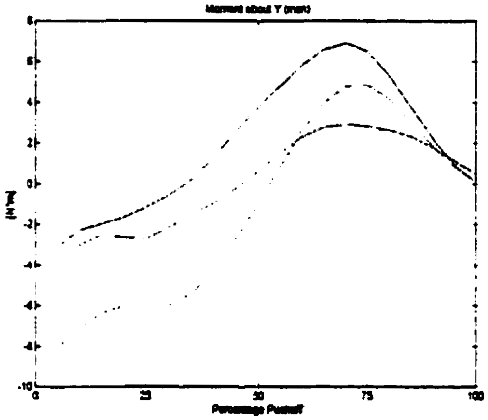

Figure 3.7a: Moment Y Axis -Men

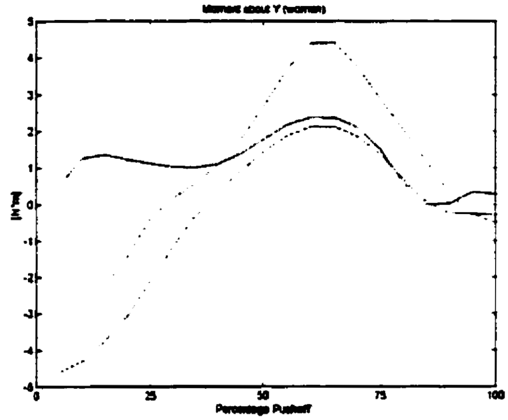

Figure 3.7b: Moment Y Axis -Women

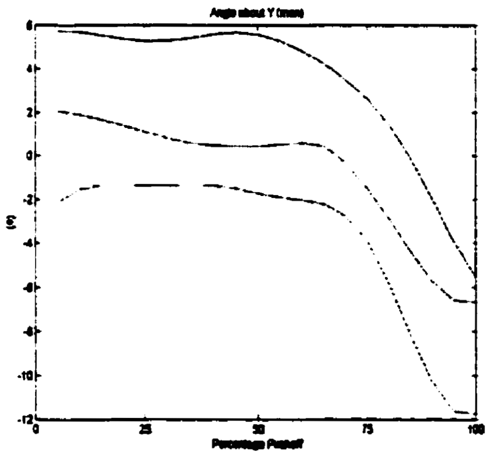

Figure 3.8a: Angle Y Axis -Men

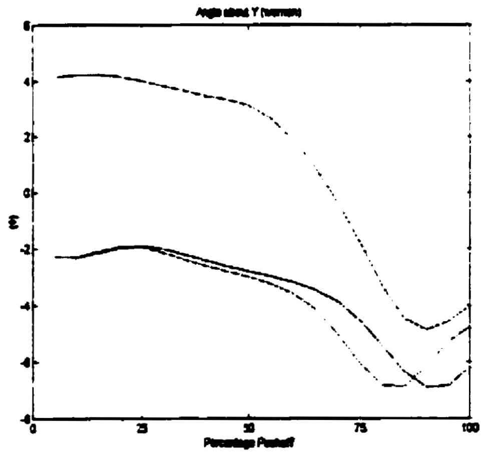

Figure 3.8b: Angle Y Axis -Women

3.3.3 X-Axis

The forces corresponding to the X axis are those which will contribute to the moments about the Y and Z axes. The forces along the X axis are those which drive the forward motion during running. Figures 3.9a and 3.9b show the force along X is approximately 0 towards the beginning of pushoff and continues to increase to magnitudes exceeding 350 and 250 N at 60 percent pushoff for men and women respectively. It may be conjectured that the force required to push the body forward is achieved mainly in this region of pushoff.

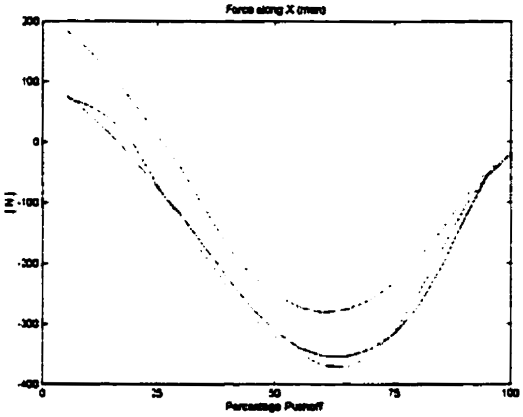

Figure 3.9a: Force X Axis -Men

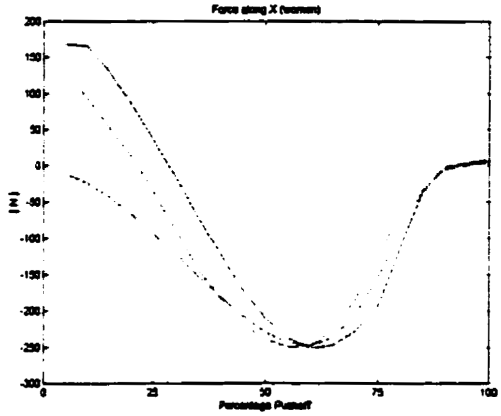

Figure 3.9b: Force X Axis -Women

Any angle deflection about the X axis will be either inversion or eversion. We note that in the push off stages of the gait cycle, eversion occurs about the entire foot with respect to the ground, which is one property of supination. However, the data obtained is of the forefoot with respect to the rearfoot. Figures 3.10 show that the forefoot is actually in an inversion trend during the entire push off stage. This is due to the rotation about the ankle, which is the principal contributor to the eversion of the foot. The foot is actually everting with respect to the ground, yet the MP joint, being stiffer about this axis, is not complying with the entire motion, thus causing an inversion with respect to the rearfoot and reaching final values between 15 and 17 degrees. In other words, the rearfoot is in a state of eversion and though the forefoot is in eversion with respect to the body, it is not everting as much as the rearfoot causing a relative inversion.

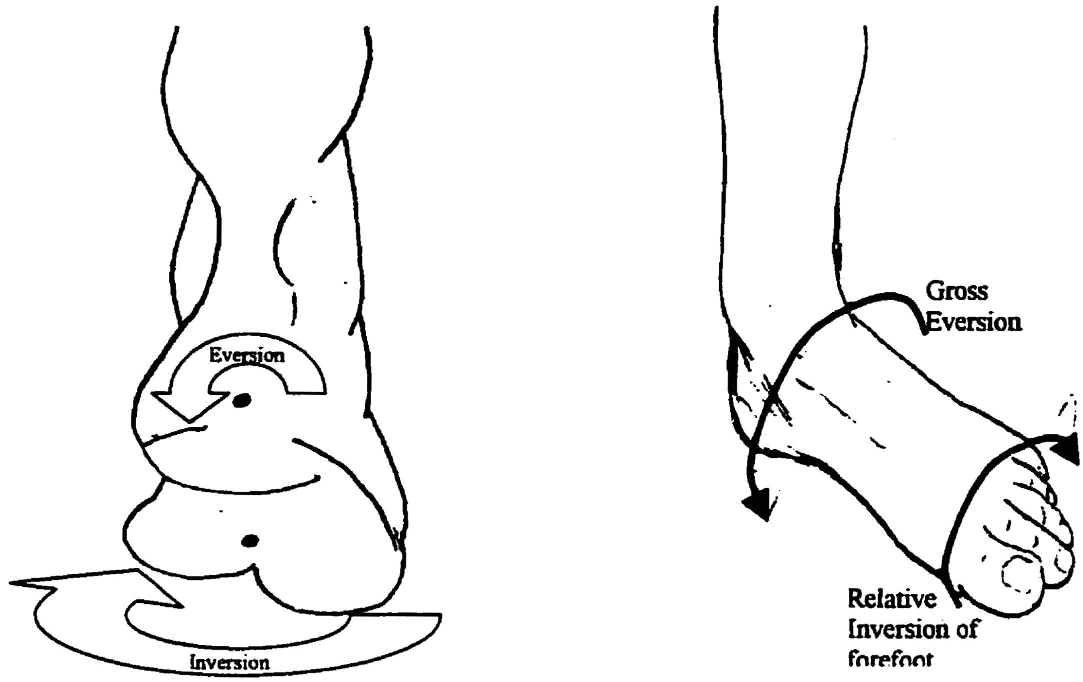

Figure 3.10: Inversion of the Forefoot

The moment calculations about the X axis for each subject, shown in Figure 3.11a and 3.11b, resulted in fairly predictable and repeatable results reaching maximums of 17 Nm and 10 Nm for men and women respectively. However, as with the previous 2 axis, the moment's amplitude begins to decrease at 50 percent pushoff while the angle of rotation, shown in Figures 3.12a and 3.12b, continue to increase. These results will cause non-linearities in the stiffness model.

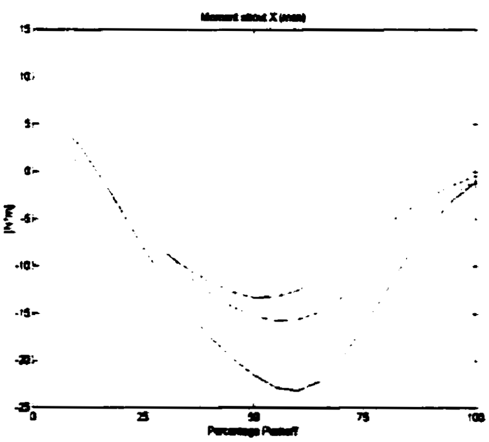

Figure 3.11a: Moment X Axis –Men

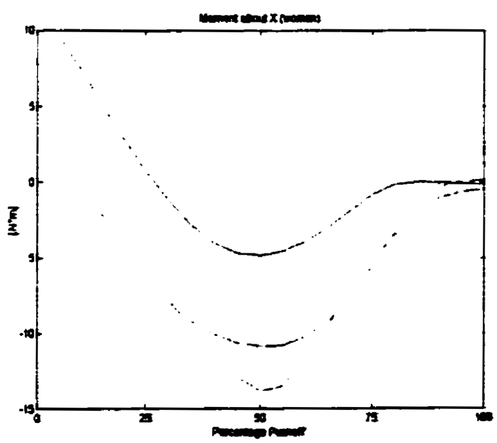

Figure 3.11b: Moment X Axis -Women

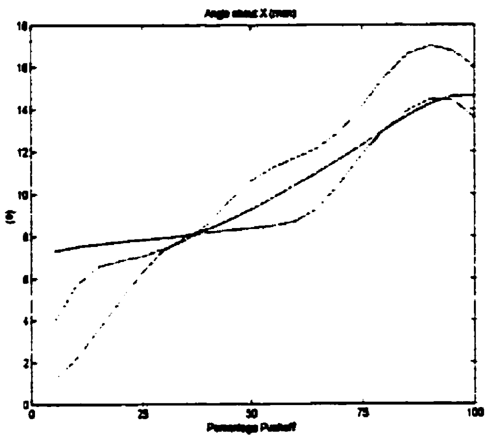

Figure 3.12a: Angle X Axis -Men

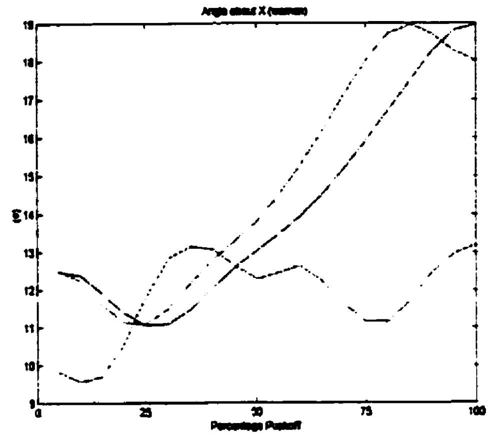

Figure 3.12b: Angle X Axis -Women

3.4 Discussion and Stiffness Analysis

The objective of these experiments was to determine the relative stiffness of the metatarsophalangeal joints about each the X, Y, and Z axis. This stiffness will be based on the moment required to produce a given angle of deflection. As for a torsional spring, a constant multiplied by the deflection will result in the force applied. The relative movements in which this experiment has observed are those of in-eversion, ab-adduction, and dorsi-plantarflexion referring to rotations about the X, Y, and Z axis respectively. The following section will extract the moment and angle information provided in Section 3.3, and will derive a stiffness coefficient about each axis as was done by Stefanyshyn and Nigg (1998). However, the stiffness about the defined axis is expected to change due to the non-linear relationship shown in Section 3.3. Thus, we define a series of 'time varying stiffness coefficients', *K(n)*, corresponding to each set of Absolute Moment/Angle data obtained:

$$K(n) = \frac{M(n)}{\theta(n)}, \tag{3.4}$$

where $n=1:n_{max}$ is the time index,
M(n) is the moment,
$\theta(n)$ is the change in angle from the neutral position.

3.4.1 Stiffness about the Z Axis

Dorsi-plantar flexion is the primary movement of the MP joint that allows for a push-off phase within the gait cycle. As mentioned, this axis is defined here as the Z-axis and extends beyond the segment connecting the 1st and 5th metatarsophalangeal joints. In referring to Figures 3.13a and 3.13b, it may be shown that the forefoot is already in dorsiflexion before the moment is applied. This may be due to the weight bearing of the sesamoid located behind the MP joint axis and will be discussed in Section 3.5. Due to this initial angle, our stiffness coefficient will only be defined for angles greater than 7 and 4 degrees into dorsiflexion for men and women respectively. An additional note is to recognize that the men seem to have greater dorsiflexion, reaching up to 38 degrees, as expected from Section 3.3, and the angle seems to quickly swing back towards the neutral position immediately after the pushoff phase. The results of the men's and women's data is quite similar, they only differ in that the moment of men is greater, creating a larger angle deflection. This is due obviously to the mean weight difference between the two gender groups.

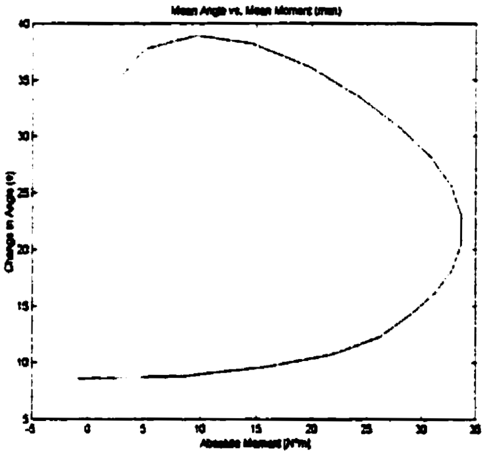

Figure 3.13a: Moments vs. Dorsiflexion (men)

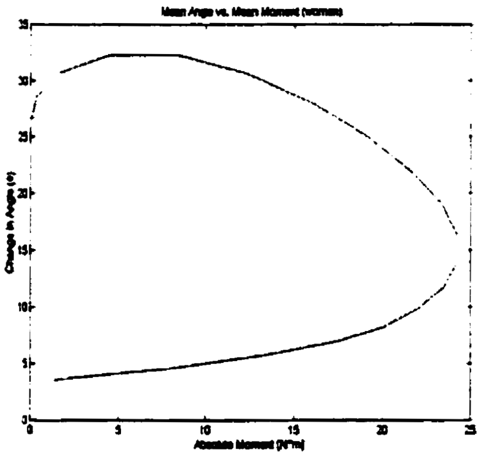

Figure 3.13b: Moments vs. Dorsiflexion (women)

Figures 3.14a and 3.14b show that the stiffness difference between men and women are relatively slight, the men reaching above 2.1 Nm/deg and the women just below 2.5 Nm/deg. However, this difference does indicate that the stiffness of the women's joint is greater, even with a smaller moment due to load. Appendix A shows the standard deviations for men's and women's stiffness. Figures 3.14a and 3.14b also provide values and stiffness trends as the angle of deflection changes. The stiffness reaches a maximum within the first 7 to 12 degrees of dorsiflexion before slowly dropping down to a zero value. These values indicate that the toes are stiffer likely due to the stiffness created during the firing of the muscles, before reverting to a more passive cantilever, which flexes as the moment increases. An interesting characteristic about this curve is that in some cases there are 2 different stiffness values for the same angle. This implies that stiffness is not dependent on the angle of the forefoot but instead is time dependent. In these graphs, the point closest to the graph's origin represents 0 percent pushoff and as the curve progresses, so does the time scale upon which these events took place.

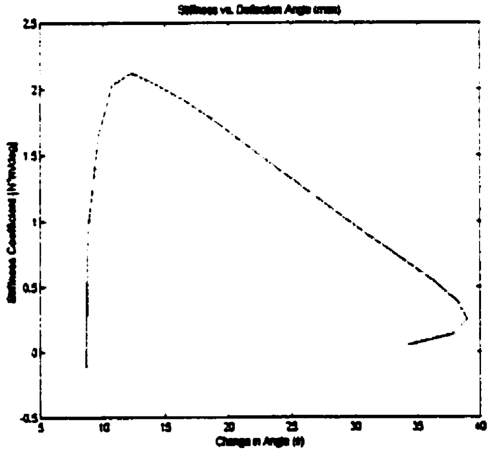

Figure 3.14a: Stiffness in Dorsiflexion

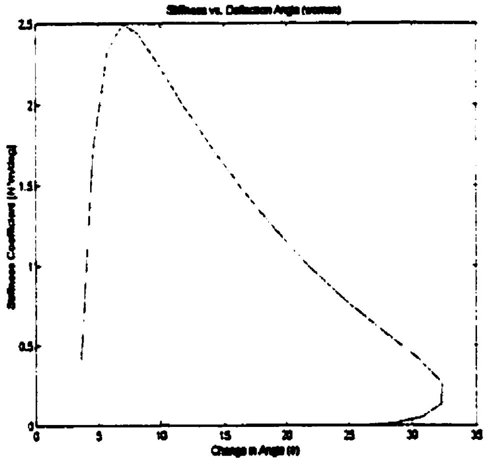

Figure 3.14b: Stiffness in Dorsiflexion

3.4.2 Stiffness about the Y-Axis

The stiffness about the Y axis is a direct product of the moments and forces tangential to the ground. One may observe the moment trend as the angle changes from adduction through abduction in Figures 3.15a and 3.15b.

Since the definition of a stiffness coefficient is the moment divided by the total angle deflection, the Y axis is fairly difficult to analyze due to the infinite results one obtains when the angle passes through the neutral position. One error is that the crossing of the rotational axis from adduction to abduction must approach and pass zero, and thus appear to create infinite stiffness as the angle approaches the neutral position. In observing Figure 3.8, one immediately notices that the angle of deflection hovers about the neutral position until approximately 70 percent of the event time. Since a stiffness value can not be attributed to a zero value, Figures 3.16a, and b commence at approximately 70 percent pushoff. Figures 3.16a and 3.16b, show that as abduction commences, which is about 25 percent of the final 30 percent of the push off phase, the stiffness increases quite dramatically, but as the angle of abduction increases beyond 2 to 4 degrees, the stiffness decreases again to a near zero position. Many authors such as Frechet et al (1996) and Lee (1997) have described abduction as resembling a spring mechanism, which varies in stiffness as deflection increases. Following this theory, it may be conjectured that during pushoff, the taughtness of the ligaments, and the added stiffness of regional muscles being fired, change the properties of the spring mechanism in question.

The maximum amount of deflection occurring during running was 8 and 6 degrees for the men and women respectively, yet once again, the women seem to have a slightly higher stiffness coefficient than the men. The standard deviations for the men's and women's stiffness may be found in Appendix A. The standard deviations of the stiffness values are significantly greater than the moment deviations due to the small angles which are used as the denominator in the stiffness calculation. Small errors in the angles could offset the stiffness values by orders of magnitude. The limitations placed on the deflection angle seem to be based mainly on the strong short plantar ligaments (Bojsen-Moller, 1979), and the literature does not indicate that gender is a factor in angular deflection limits.

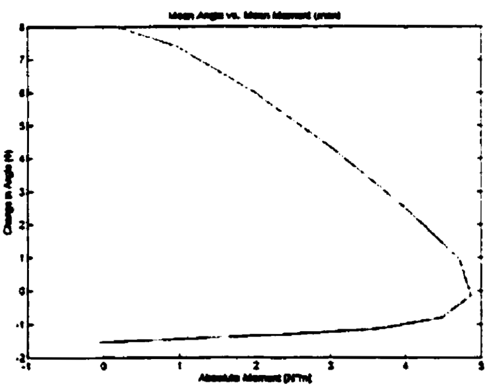

Figure 3.15a: Moment vs. Abduction-men

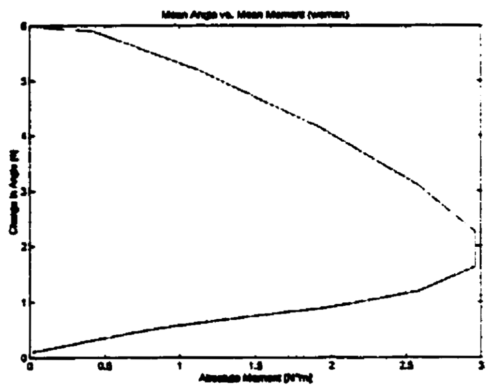

Figure 3.15b: Moment vs. Abduction-women

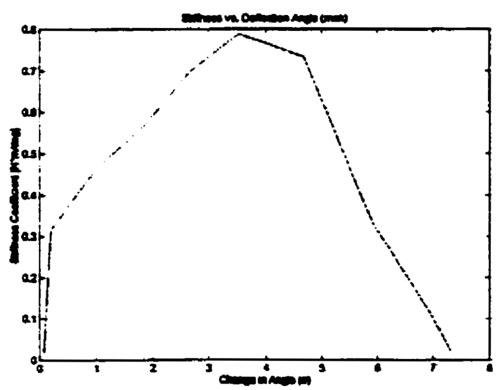

Figure 3.16a: Stiffness vs. Abduction Angle

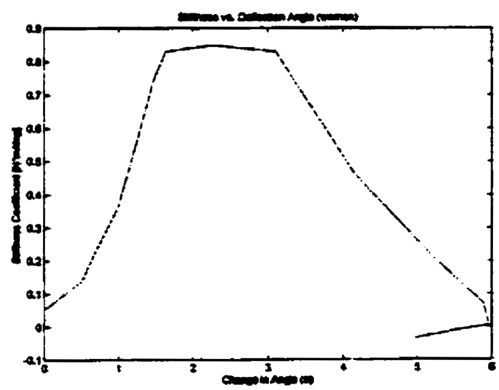

Figure 3.16b: Stiffness vs. Abduction Angle

3.4.3 Stiffness about the X-Axis

Figures 3.17, 3.18, a and b, show the moment, and stiffness curves relating to angle deflection during push off. The MP joint is in a state of relative inversion due to the eversion created by the ankle. When the push off stage commences, there is already an angle deflection with respect to the neutral position. As with the other axes of rotations, the stiffness increases initially, yet proceeds to drop to a lower coefficient. The stiffness for the men reaches its maximum at 10 degrees while the women reach maximum stiffness at 13 degrees. Once again, this data implies that the stiffness of the MP joint changes quite significantly during push off, likely due to the change in associated muscular activity throughout this stage. Appendix A shows the Standard Deviations for the stiffness curves.

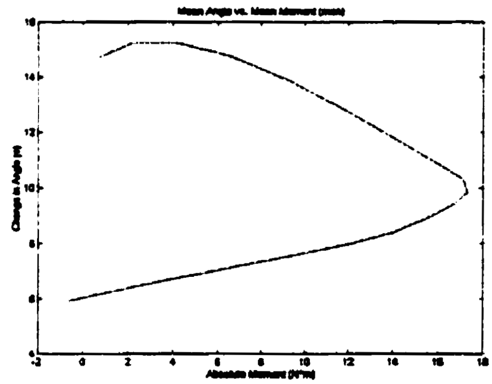

Figure 3.17a:Moment vs. Inversion(men)

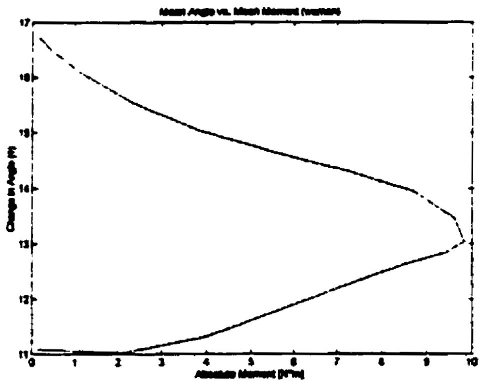

Figure 3.17b:Moment vs. Inversion(women)

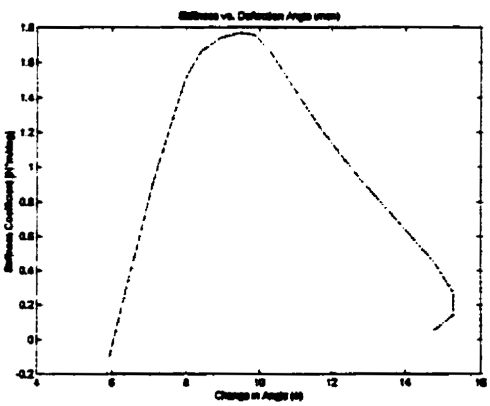

Figure 3.18a: Stiffness vs. Inversion (men)

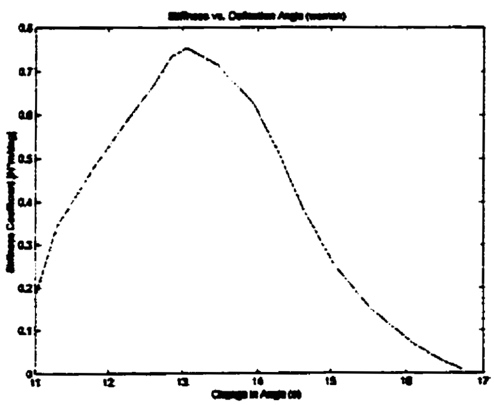

Figure 3.18b: Stiffness vs. Inversion(women)

3.5 Discussion on Repeatability and Potential Errors

In this chapter, an analysis of human gait was observed in order to quantify a stiffness coefficient about the metatarsophalangeal joint. This experiment provided a basic understanding of the human MP stiffness, but it must be noted that there are deviations within the results. The intra-subject standard deviations shown in Table 3.2, are based on the average of the 10 trials taken per subject. The mean standard error is not included due to the moment passing from negative to positive values, resulting in an infinite error as the mean value approaches 0. Alternatively the standard deviations are also expressed as a percentage of the total range and may be found in Appendix A. The validity of the data may be shown by the standard deviations of the moment data since the stiffness is simply a function of the moment. However the standard deviations of the stiffness are much greater than the moment deviations due to the deviations within the angle data whose values are small enough that the slightest error may offset the stiffness values by orders of magnitude.

Subjects	σx Mean Std. Dev. (X)	σx / Range	σy Mean Std. Dev. (Y)	σy / Range	σz Mean Std. Dev. (Z)	σz / Range
Subject 1	1.74E+00	5.91E-02	1.38E+00	1.15E-01	2.47E+00	7.50E-02
Subject 2	3.61E+00	1.22E-01	1.82E+00	1.52E-01	3.72E+00	1.13E-01
Subject 3	2.48E+00	8.41E-02	1.11E+00	9.26E-02	2.97E+00	9.01E-02
Subject 4	3.68E+00	1.25E-01	1.97E+00	1.64E-01	3.46E+00	1.05E-01
Subject 5	2.09E+00	7.09E-02	9.98E-01	8.32E-02	1.81E+00	5.48E-02
Subject 6	2.29E+00	7.75E-02	8.57E-01	7.14E-02	3.67E+00	1.11E-01
Subject 7	2.05E+00	6.94E-02	8.30E-01	6.92E-02	2.58E+00	7.81E-02
Subject 8	1.96E+00	6.64E-02	1.10E+00	9.18E-02	2.00E+00	6.05E-02

Subjects 1:4 = Male Subjects 5:8 = Female

Table 3.2: Intra-Subject Moment Standard Deviations

The intra-subject data is quite repeatable per subject, as shown by Table 3.2, and the shape of the curves provides more evidence of this repeatability. Figure 3.19 shows the non-normalized moment graph for the 10 trials of 'Subject 1', and though there are deviations within the values, each curve demonstrates the same shape occurring at similar times.

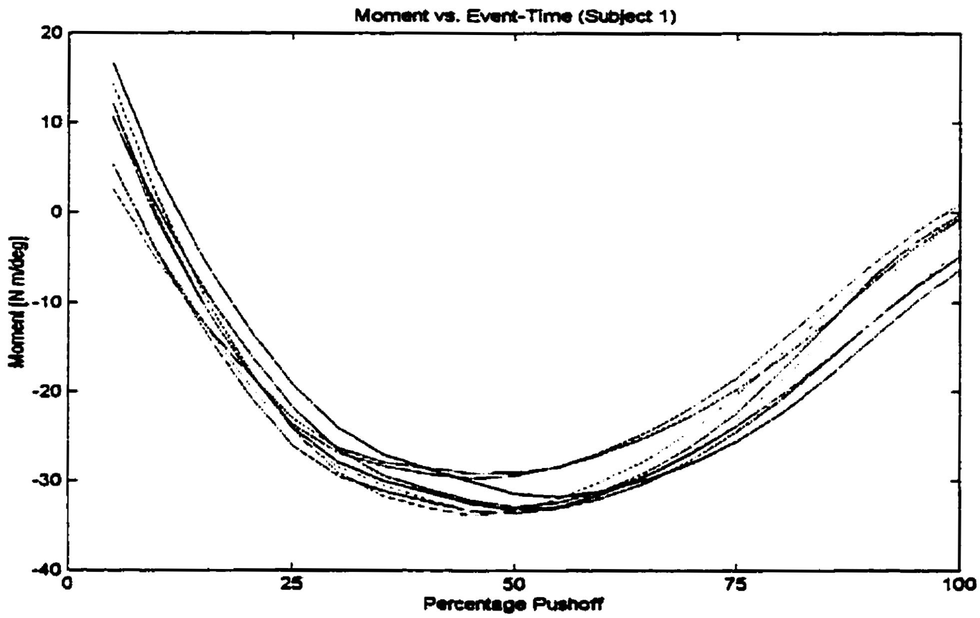

Figure 3.19: Non-Normalized, Intra Subject (1) Moment Data

The standard deviations, shown in Table 3.3, are based on the inter-subject data as opposed to the intra-subject data trials presented earlier. The repeatability of the data is less between each subject than within each subject's trials. This is expected since a subject's gait differs from individual to individual.

Gender	σx (ave)	σx / Range	σy (ave)	σy / Range	σz (ave)	σz / Range
Male	3.1504	0.0955	1.924	0.1282	2.258	0.0594
Female	3.2708	0.1258	1.156	0.1284	2.366	0.0709

Table 3.3: Inter Subject Standard Deviations

The standard deviations for the moment about the Z axis are quite low at 6 and 7 percent of the range of the existing moments. The magnitudes of the standard deviations may be relatively high at times for the X and Y axes, however the force and angle curves shown in the previous sections of this chapter are relatively repeatable. The weight of the individual and the style in which they run are the greatest factors that prohibit high repeatability within the data about these 2 axes. This data shows that there is a greater consistency and repeatability between subjects about the Z axis while the X and Y axis demonstrate less repeatable data. Therefore, it may be conjectured based on the data, that the magnitude of in-eversion and ad-abduction are more a factor of a runner's style than that of dorsi-plantarflexion.

In addition to the repeatability of the data, there may be unknown potential errors in the data caused mainly by weight bearing of the rearfoot and the sesamoid located posterior to the MP joint axis. If the foot is modeled as two rigid bodies, as shown in Figure 3.20, the force being exerted on the rearfoot should not produce flexion of the forefoot. However, the calculated moment from the data is influenced by the forces behind the MP joint which results in a measured forefoot moment M'_f which, assuming a negligable moment of inertia, is the summation of the rearfoot moment M_r and the true forefoot moment M_f. Since these moments are in the opposite directions, the forefoot moment M'_f will be less than the actual forefoot moment M_f.

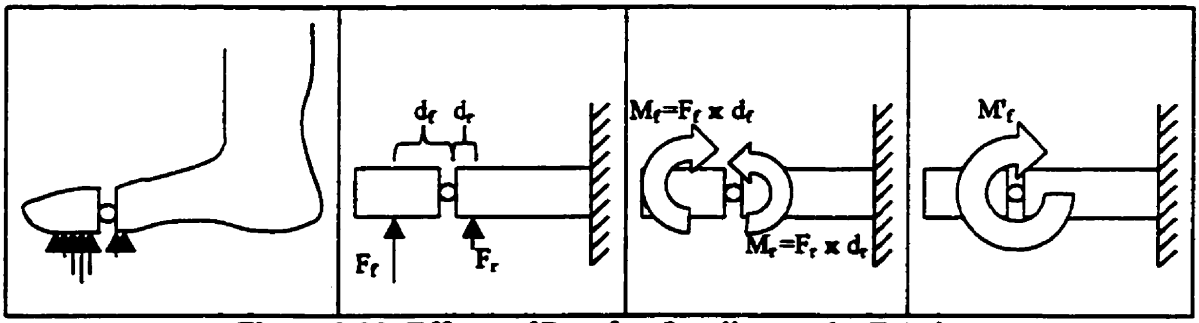

Figure 3.20: Effects of Rearfoot Loading on the Z Axis

Research by Stefanyshyn and Nigg, who quantified moments about the MP joint, indicated that the ground reaction forces should, ideally, be divided into two forces, each corresponding to a point of application on either side of the metatarsophalangeal joint (Stefanyshyn D., Nigg B., 1997). However, in this experiment, the force plate data retrieves the centroid of the forces throughout the entire foot, which means that the force on the sesamoid and rearfoot portions may account for a portion of the moment as shown in Figure 3.21.

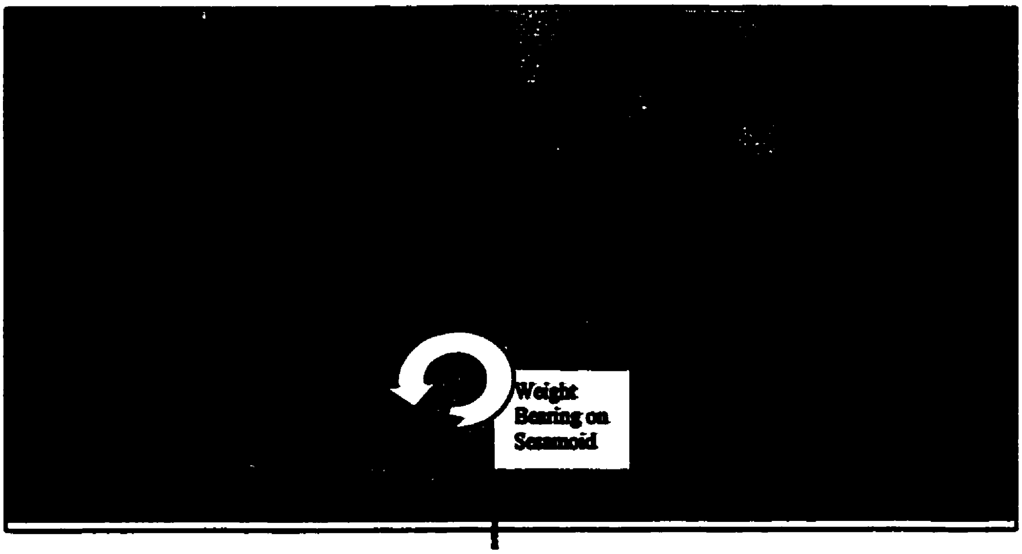

Figure 3.21: Moment caused by Sesamoid behind Z Axis

Since the sesamoid is only partially in the rearfoot portion, this minimizes the effects on the results and will likely only disturb the data in the transition between the 'stance' phase and 'pushoff'. This seems to be relatively justified by Stefanyshyn and Nigg (1997) who also calculated the difference in the joint moment data of the MP joint using both pressure insoles and force plate data. This research showed that a single ground reaction force used to determine net moments about the MP joint was acceptable and would only lead to a small underestimation of the MP joint moment.

These effects of rearfoot loading would likely not have any influence on the moments calculated for the Y axis due to its orientation. However, unlike the Z axis, the X axis may be subjected to greater errors due to the distance between the sesamoid and the X axis and may result in less repeatable data between trials. Figure 3.22 demonstrates an example of how the measured forefoot moment, M_{Tot}, may contain errors due to the forces applied to the rearfoot. The measured forefoot moment is the summation of the net forefoot moment M_F, and the net rearfoot moment M_R. The M_R portion of M_{Tot} is an error since it will not affect the forefoot motion, and unlike the Z axis, the force application is a relatively significant distance from the X axis likely causing a significant moment contribution to M_{Tot}.

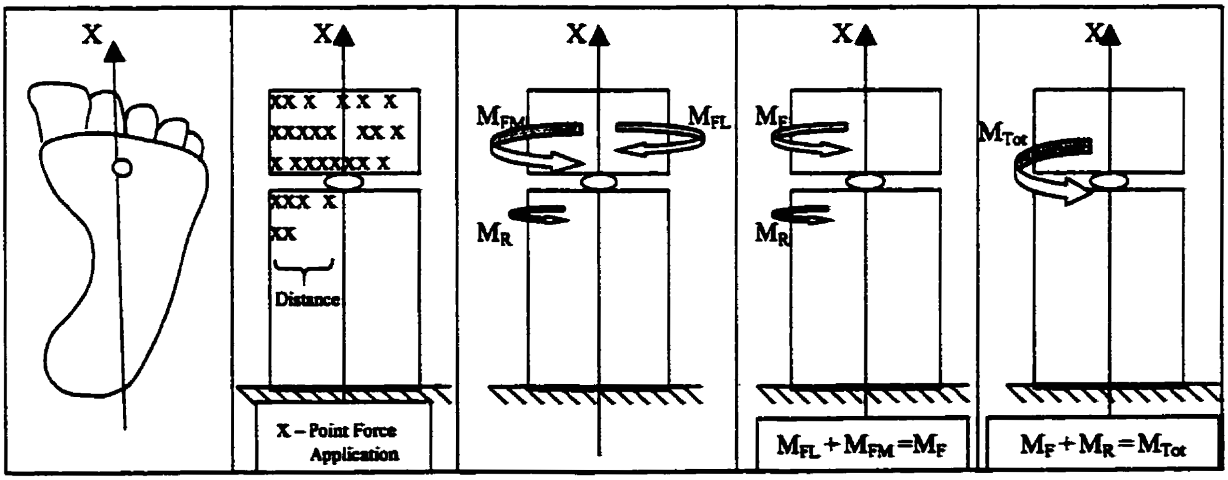

Figure 3.22: Effects of Rearfoot Loading on the X axis

3.6 Summary

The purpose of this in vivo study was to determine the relative stiffness coefficient about the three axes of the metatarsophalangeal joint segment. The joint line was defined as the extension of the 1st and 5th MP segment, which approximates the transverse and the oblique joint axes. Video and Kistler force plate data was collected for 8 subjects, tracked using Eva V5.0, and was filtered using floating points and Splines within Matlab 5.2. Neutral standing positions were defined by the relative angle between the forefoot and the ankle and were initialized to 0 degrees.

The Z-axial rotation defined the plantar-dorsiflexion rotations. The data for this axis showed a relative maximum dorsiflexion during push off of 39 and 34 degrees for men and women respectively. In addition, this maximum angle was obtained at approximately 90 percent pushoff. The moment data reached a maximum of 34 Nm and 24 Nm for men and women respectively and was reached at 50 percent pushoff. These moment values are less than the values obtained by Stefanyshyn and Nigg. This may be expected since the running speeds in this study were less than those found in the Stefanyshyn and Nigg research. The moment data resulted in a stiffness coefficient reaching a maximum of 2.1 Nm/deg and 2.5 Nm/deg, for men and women respectively at 10 to 15 degrees dorsiflexion. Abduction and adduction of the foot characterize the rotations about the vertical Y axis. As the foot approaches toe-off, the foot approaches a relative abduction state. During push off, the forefoot moves from a relatively neutral/adducted position through to an abducted position. The maximum abducted rotation of the forefoot is 8 and 6 degrees maximum moments reaching 5 Nm and 3 Nm for men and women respectively. The offset between the maximum moment and position is much smaller than that of the Z axis. However, a problem exists in determining the stiffness near 0 degrees of deflection due to the denominator of the coefficient being too small to effectively calculate an accurate value. However, the data seems to indicate that the stiffness increases up to an absolute value of 2 Nm/deg at 1 degree of rotation, but then decreases for the remainder of the abduction. Finally, inversion-eversion, which occurs due to the rotation about the X axis, results in an initial inversion state at 0 percent of push off. The inversion of the forefoot is a response to the gross eversion created about the heel side of the ankle, which is our reference frame. The maximum stiffness occurs at 10 and 13 degrees for men and women respectively, and then proceeds to decrease as is in the case of the dorsiflexion and abduction. The maximum stiffness obtained in inversion is 1.8 Nm/deg and 0.7 Nm/deg for the men and women.

If the stiffness throughout the foot's joints are a function of the surrounding tendon and muscular activity, then the stiffness of the MP joints decrease as the muscles cease firing. One possibility is that when the momentum of the body is enough to propel itself forward, the muscles relax allowing the MP joint to react passively, using the toes as simple cantilevers to roll off with. This seems to agree with established studies indicating that the toes are active in propulsion of the body (Mann, R.A & Hagy, J.L, 1979), and that they also react passively under the body's weight bearing (Bojsen-Moller & Lamoreux, 1979).

4 SHOE STIFFNESS EXPERIMENT

In this chapter, the stiffness of 3 different shoes will examined and compared with the human foot data. This will be done in order to show which axes are relevant in the prosthetic design and will simplify the modification requirements.

4.1 Overview

The stiffness about a joint connecting 2 rigid bodies, as is the case with our forefoot-rearfoot model, may be increased by adding support to the joint which connects the 2 bodies. In the case of metatarsophalangeal joint, the support affecting the stiffness is obviously the shoe. The need for flexibility within the sole of the shoe has yet to be proven scientifically (Segesser & Pforringer, 1987), but runners' preferences seem to point strongly towards the need for flexible footwear. A sport shoe is designed such that the shoe can bend at least 30 degrees at a point just behind the metatarsal heads with relative ease. Segesser et al. (1987) suggest that any additional stiffness torque required to bend a stiff shoe through this arc may result in muscular fatigue. It is also believed that toe spring creates a more efficient stride. However, Cavanagh (1980) stated that there was no evidence of this being true. In fact, research by Stefanyshyn and Nigg (1997) seems to indicate that the midsole materials at the MP joint may be too compliant.

The foot of a shoe testing robot must mimic the properties of an actual human foot, which were outlined in Chapter 3. This foot will respond passively and should be able to imitate the stiffness of its human counterpart. The previous chapter sought to determine a stiffness model of the human foot during running, while this chapter will determine the stiffness of the shoe about the same axes previously outlined. Thus, in this chapter, a stiffness analysis of 3 different shoes will be conducted and compared with the human foot data.

4.2 Methodology

4.2.1 Assumptions

In this experiment, a stiffness coefficient is to be determined about each axis. In conducting this experiment, several assumptions must be made regarding the setup and the material properties of the shoe samples.

The first assumption will be called the 'time-invariant approximation assumption'. In this experiment, the angle increments are performed relatively slowly so that accurate angle and force data may be determined. Goldsmith and Oleson (1999) conducted a study which clearly showed the difference in the force versus deflection curve between dynamic and quasi static compression. It is conjectured that this difference is due to an air capacitance effect. This air capacitance is created by the air trapped within the porous material of the shoe. When this material is compressed slowly, the air within these pores has an opportunity to escape. However, when the compression rate is higher than the diffusion rate of the air pockets, these air pockets increase the stiffness. In creating a deflection angle about a given axis in the shoe, there will be compression and tension in different levels of the shoe sole as shown in Figure 4.1. Thus, because the air has time to results in a conservative estimate of the shoe stiffness due to the neglected air capacitance effect of the shoe sole. In reality, during a running motion, the air likely not have enough time to escape in the first place resulting in a greater stiffness along the sole.

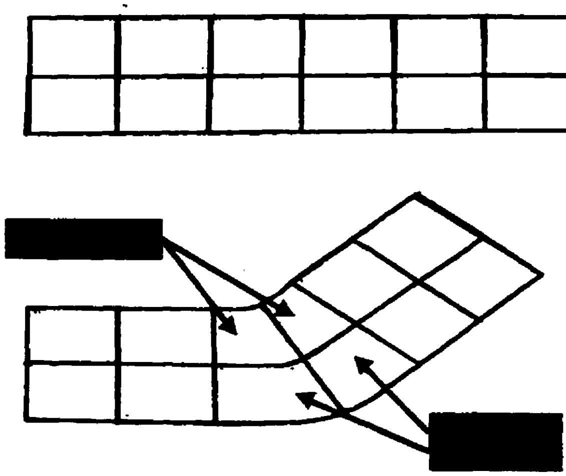

Figure 4.1: Tension-Compression through a bending beam or surface

The Second assumption is that the bending and torsion of the shoe sole occurs solely about the axes defined in Chapter 2. This assumption is reasonable due to the rigid lasts and anchors placed in the shoe which restrict motion along the sole of the shoe.

4.2.2 Shoe Samples

The samples used in this experiment were 3 Adidas (Adi-Dassler-Str 24-26, 91443 Sheinfeld, Germany) running shoes. All shoes were new and had not been used prior to the experiment. As will be discussed in Section 4.2.3, each shoe was anchored to 'lasts' approximately 8.9 centimeters apart. One of the lasts was connected to a rigid fixture thus maintaining a reference frame such that one could measure the angles of deflection. The material and laces were cut along the tongue line and around the forefoot section such that material and laces were cut along the tongue line and around the forefoot section such that the material would not interfere with the anchoring bolts. Table 4.1 contains additional information about each of the shoes used. Each shoe was tested only once but the force was sampled 10 times for every angle. The shoe was not tested again due to possible plastic deformations which likely occurred during the experiment.

	Manufacturer	Type	Size	Design Period	Model
Shoe 1	Adidas	Torsion	9	Recent	033756
Shoe 2	Adidas	Torsion	9	Less Recent	033756
Shoe 3	Adidas	Orig. Running	9	Old	428803

Table 4.1: Running Shoes Tested

4.2.3 Setup

This experiment was performed using a combination of the MTS machine model 510.10C, a 10 gpm pump, an MTS hydraulic service manifold model 293.11B-01, a linear actuator model 242.02, series 252 servovalves, and an MTS axial force transducer model 661.19E-01 with a working limit of $\pm$5000.00 Newtons. This setup is located at the Calgary Health Sciences Center and was supervised by the University of Calgary's Health Science Staff.

The experiment was performed using 1 degree of translational freedom but generated a 1 degree of rotational freedom reaction. The MTS machine was placed under position control and was able to provide force measurements along a vertical axis. The position increments of the MTS were controlled using Testware SX 4.0c software from a PC computer. For the Z-axis, two rigid metal plates were connected directly to the interior the Z-Axis, as shown in Figure 4.2. Similar plates were used to isolate the X and Y axes independently.

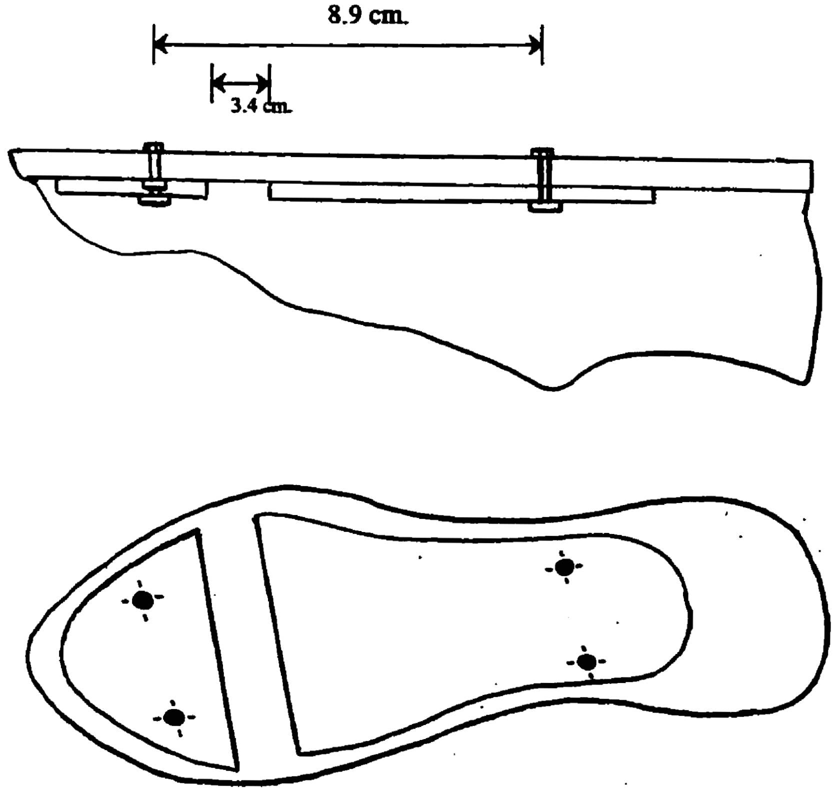

FIGURE 4.2: Shoe and Lasts (Z-Axis)

In order to duplicate the rotation of the shoe while still maintain conservative estimates, the plates were connected to the shoes by 2 anchoring bolts, laterally placed such that a secured separation between the forefoot and rearfoot existed. Due to the width of the plates, the distance between the 2 plates were determined by the minimum separation that could occur without the plates coming into contact at maximum dorsiflexion. This distance will provide the results with a high estimate for the stiffness. The rear last was connected to a solid fixture and was set to 0 degrees using a revolving joint of the fixture. The front last was connected to measuring beams equipped with protractors such that the

The front last was connected to measuring beams equipped with protractors such that the angle of rotation may be easily retrieved with respect to the rearfoot. The fixture orientation is shown pictorially in Figures 4.3 a, c and d for the Z, X and Y axis respectively and is shown schematically for the Z axis in Figure 4.3 b. Note that Figure 4.3d the measuring bar is not shown.

FIGURE 4.3a: Fixture for Z-Axis

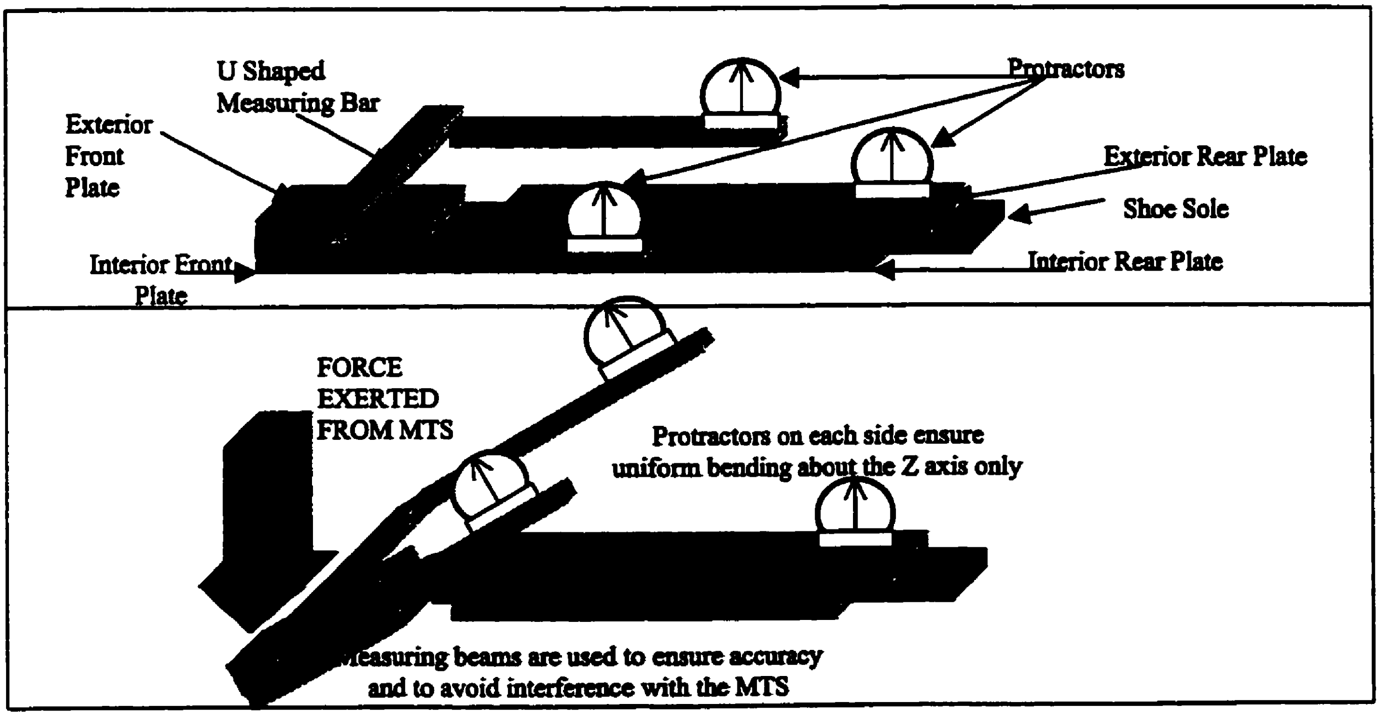

FIGURE 4.3b: Fixture for Z-Axis

FIGURE 4.3c: Fixture for X-Axis

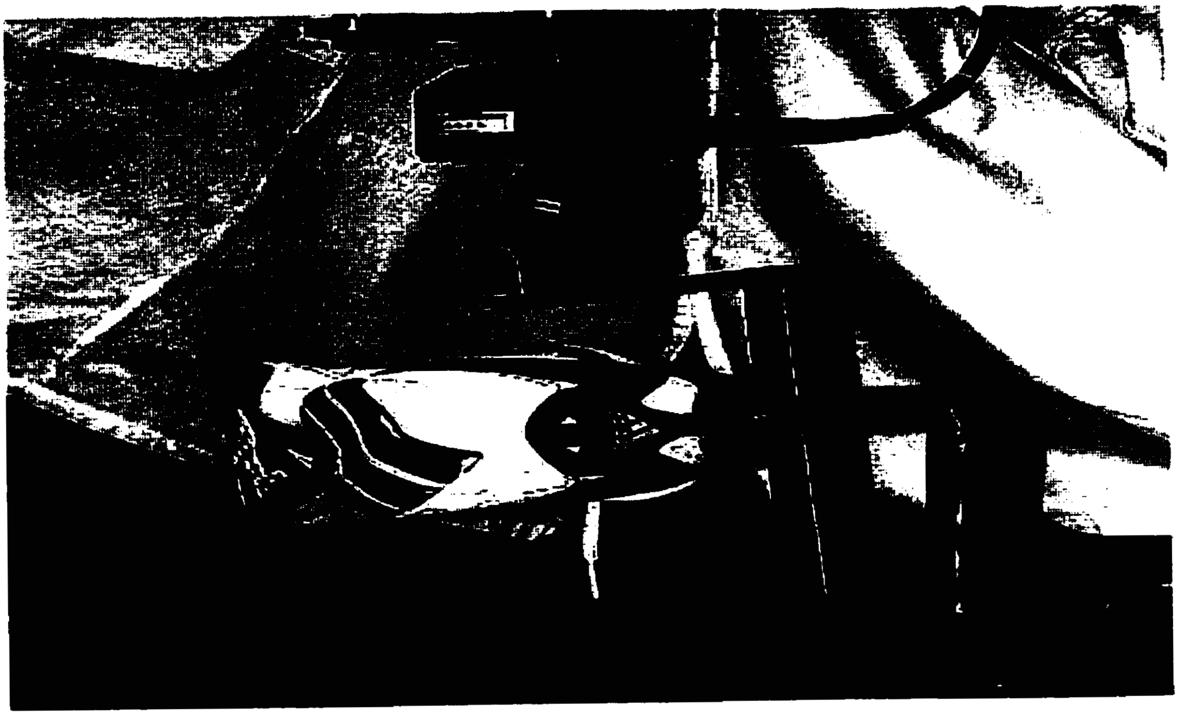

FIGURE 4.3d: Fixture for Y-Axis

4.2.4 Procedure

The actuator of the MTS moved in a step function, and then sampled the resultant force over 5 seconds. Since the actuator was stopped before taking the measurements the acceleration of the end effector was removed from the force calculation. This additional time allowed the user to verify the angle retrieved from the shoe-fixed protractor.

The actuator moved to the next position dictated by the step-position control program. The distance traveled between steps varied, depending on the axis to be tested. The X and Y axes have smaller position increments of 1 mm ($\pm$.005)' due to the size of the lever arm upon which the force is applied. The Z axis, having a much larger lever arm, had 2.5 mm of travel between each step. This was done to reduce redundant data collection due to the small angle increments, resulting from a displacement and motion applied to a larger lever arm.

Minor geometric manipulations and transformations are required such that the vertical direction and force data of the actuator may be related to the resultant rotation about the desired axis of the shoe. Since the actuator stops before sampling the force data, the force due to damping or any change in acceleration of the end effector converges to zero before the data is gathered. The force due to gravity of the end effector is accounted for before commencing the experiment.

Using basic trigonometric manipulations, the force exerted on the shoe may be calculated. Similarly, the equation for the moment will undergo changes due to the incremental change in distance from the force application relative to the joint center. Figure 4.4 shows how the distance from the rotational axis changes as the actuator moves vertically. In addition, the force that is recorded by the MTS is only the vertical force. The horizontal component to the force must be calculated as shown and increases as the shoe undergoes further rotation.

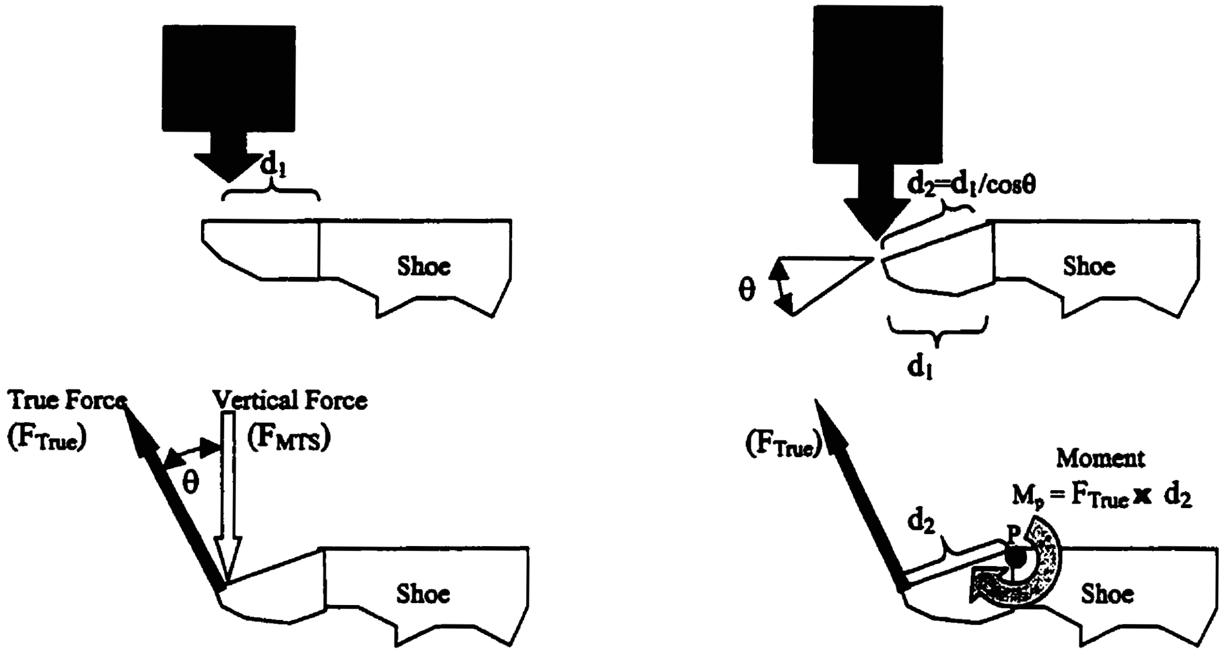

Figure 4.4: True Angle, True Force and the Resultant Moment

Since the MTS force sensor measures forces along the vertical axis, it is necessary to determine the true resultant force exerted by the shoe. The rotational portion creates a horizontal force component as soon as the rotation about any MP axis exceeds 0 degrees. Thus we must determine F_{True} from Equation 4.1, d_2 from Equation 4.2 and apply them to Equation 4.3 in order to determine the moment about P.

$$F_{True} = \frac{F_{MTS}}{\cos\theta} \tag{4.1}$$

$$d_2 = \frac{d_1}{\cos\theta} \tag{4.2}$$

$$M_p = F_{True} \cdot d_2 = \frac{F_{MTS} \cdot d_1}{\cos^2 \theta} \tag{4.3}$$

Where θ is the angle of deflection with respect to the rear portion of the shoe.

Since the experiment had the potential of causing plastic deformation in the shoe, each shoe was tested only once in the material testing machine, however 10 force samples were taken per iteration, which were averaged in order to obtain one discrete value per iteration. The data was processed using MATLAB splines and TestwareSX 4.0c (Eden Prairie, Minnesota).

4.3 Results and Discussion

In this section we will compare the stiffness results of the shoe with the stiffness of the foot in order to determine which is dominant through the motion. This comparison will suggest that the Z axis is most important when modifying and or designing the prosthetic foot.

4.3.1 Stiffness about the Z-Axis

The rotation about the Z axis of the shoe is extremely important and is essential in allowing dorsiflexion of the forefoot. Figure 4.5 shows the graphs of each shoe where stiffness is plotted against angle of dorsiflexion.

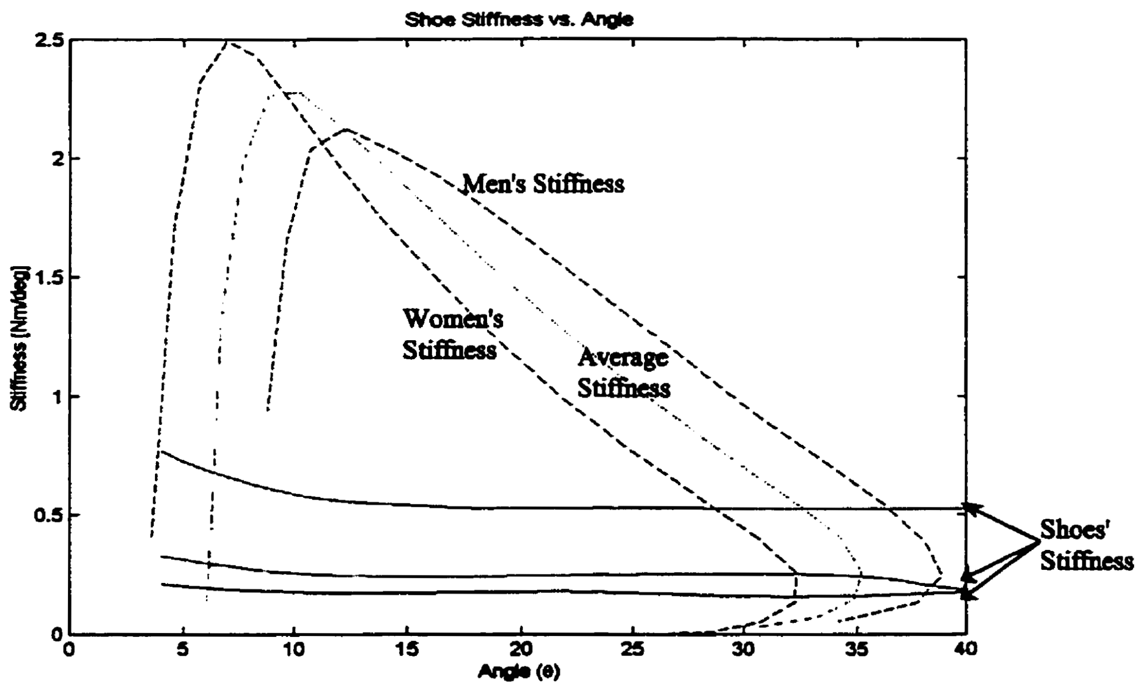

Figure 4.5: Z Axis - Shoe Stiffness versus Angle

The first observation is that the stiffness of the shoes seems to be constant through the motion applied. Though the intra-shoe data was extremely repeatable, the inter-shoe data clearly shows that each shoe has a different stiffness ranging from just above 0.2 Nm/deg to just below 0.5 Nm/deg for the entire range of motion.

In our human mechanical model based on Chapter 3, the angular range is approximately 7 to 39 degrees and 4 to 33 degrees for men and women respectively, as shown in Figure 4.5. In using the shoe with the greatest stiffness, a comparison between the human stiffness and the shoe is made which shows that the stiffness of the human is greater than the shoe stiffness for most of the range occurring from 7 to 35 degrees. The shoe with the least amount of stiffness has a lower stiffness coefficient than the foot for the majority of the range of motion throughout push-off. Only towards toe-off is the human foot stiffness lower than that of the shoe. This indicates that the shoe stiffness has a very small influence in determining the range of dorsiflexion about the metatarsophalangeal joints. This is a good feature in a running shoe, as suggested by Segesser and Pforringer (1987). Their research claims that flexibility about the Z axis, defined in this case by the vector connecting the 1st and 5th metatarsal head, is an extremely good attribute of a well made running shoe, and reduces the potential for muscular strain and injury.

The fact that the shoe is so compliant about the MP axis also supports Stefanyshyn's (1997) conclusion that this axis may be overly compliant. Regardless, this has shown that foot stiffness about the Z axis of the foot is obviously an important factor and must be included in the requirements of the prosthetic.

4.3.2 Stiffness about the X-Axis

The X axis of the shoe has a much different role than that of the Z axis. Its main role seems to be for the allowance of inversion and eversion of the front foot to occur, while providing torsional stiffness. Figure 4.6 shows that the stiffness ranges from approximately 0.2 Nm/deg to 0.7 Nm/deg depending on the shoe. However, the data from each shoe shows that the stiffness is nearly constant throughout the desired motion.

First, in comparing the men's results with the shoe data, it is shown by Figures 3.18a and 4.6 that the stiffness of the foot exceeds that of the shoes' maximum and minimum stiffness values for the ranges 7 to 14 degrees, and 6 to 15 degrees respectively. However in the women's data shown in Figures 3.18b, the shoes with the max and min stiffness of

Figure 4.6, are only exceeded by the human foot stiffness for the ranges 12.5 to 13.5 degrees and 11 to 15 degrees respectively.

The data would seem to indicate that the shoe stiffness plays a relatively important role about this axis, especially in the female gait. However, the accuracy of this data may be in question due to the small angle deflections which the foot moves, with respect to the human test errors. It may be difficult to be conclusive as to the effect of the sole on eversion and inversion. In addition, research by Xia and Robinson (1989) on athletic lateral stability seemed to indicate that shoe torsion may not even correlate to the associated forefoot torsion inside the shoe about the X axis. Though the shoe stiffness exceeds that of the foot for only approximately 50 percent of the pushoff time, it's small angular range results in a level of importance less than that of the Z axis. Despite the lack of research supporting the relationship between the torsion of the foot and shoe about this particular axis, it would be ideal to modify the prosthetic such that future work may focus on determining the stiffness about the X axis.

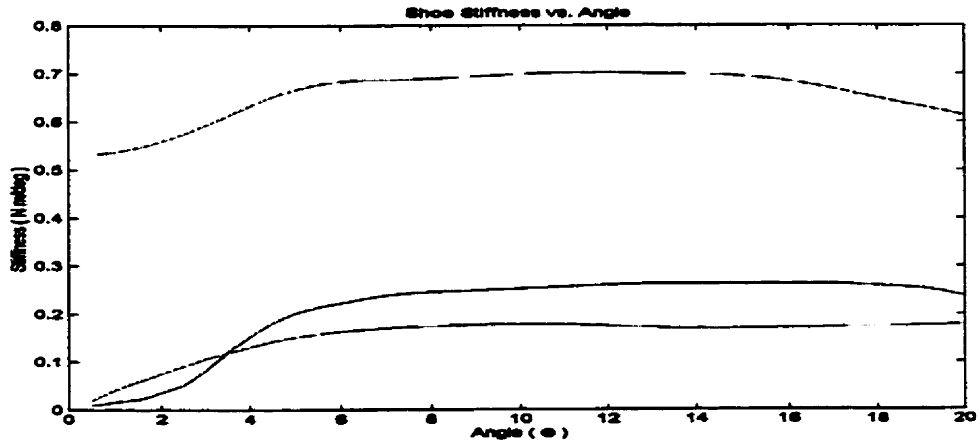

Figure 4.6: X Axis - Shoe Stiffness versus Angle

4.3.3 Stiffness about the Y-Axis

The stiffness about the Y axis demonstrates how the shoe responds to horizontal force applications resulting in ab-adduction. Figure 4.7 shows that the stiffness is constant through a very long range of motion, and that the stiffness values are of magnitude 1.2, 0.5, and 1 Nm/deg for shoes 1, 2 and 3 respectively.

The rotation about the Y axis of the forefoot with respect to the rearfoot is clearly an abduction motion for the human subject during pushoff. For this reason, the forefoot portion of the shoe was only rotated to correspond with an abducting motion. In comparing the results from the shoe stiffness with that of the human stiffness, it may be shown in Figures 3.16 and 4.7 that the stiffness constants of the shoes range between 1.2 Nm/deg and 0.5 Nm/deg. With these values, the shoe stiffness dominates the stiffness in angles exceeding 2 and 3 degrees for men and women respectively for the stiffer shoe, and 5 and 4 degrees under the same criteria using the less stiff shoe.

As shown in Chapter 3, the amount of ab-adduction that occurs during running is relatively insignificant compared to the errors and the amount the foot likely moves within the shoe. It is also conjectured that the compliance of the material in the shoe may allow for such compliance regardless of the sole stiffness since it is along the X-Z plane, which is constrained only by the shoe material, and not the sole.

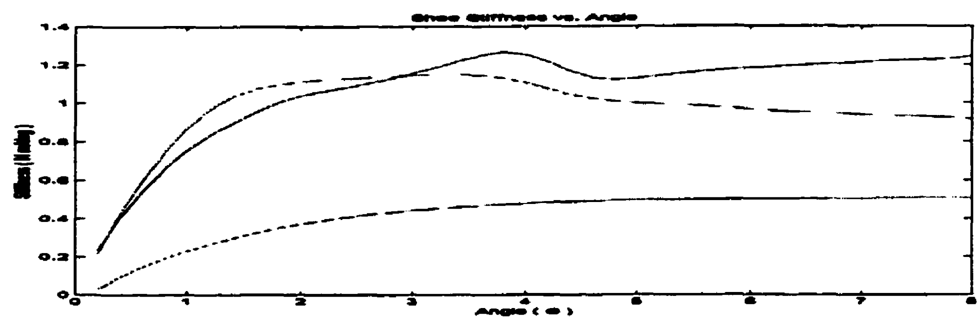

Figure 4.7: Y Axis - Shoe Stiffness versus Angle

4.4 Summary

The purpose of this shoe stiffness study was to quantify the stiffness coefficients of a running shoe sole, to compare them with the stiffness coefficients exhibited by the human foot, and to determine, based on a comparative analysis, whether a particular axis should be included in an artificial foot model. The shoe tests showed that the stiffness of the foot was dominant about the X and Y axes for the ranges between 1 and 4 degrees, and 2 to 5 degrees respectively. The variance in the data was dependent on the gender of the subject, and the particular stiffness of the shoe being used. The shoe's stiffness dominates the ranges exceeding these angles, and slippage of the vertical actuator on the shoe sole may account for these small angle deflections without affecting the shoe sole itself. Therefore, based on the errors in calculating stiffness about small deflections, and the repeatability of the human data, these 2 axes will not be the focus of the modification in the foot model. However, the foot's Z axis, which undergoes the primary 'pushoff' motion, was shown to be much stiffer than the shoe stiffness for the majority of the angular range. This axis will be the focus of the modifications to the prosthetic foot due to its dominant stiffness, and its importance to this particular stage of the gait cycle.

5 PROSTHETIC FOOT STIFFNESS

The objective of this chapter is to measure the stiffness coefficients of a prosthetic foot and to determine how close the prosthetic approximates the human joint stiffness. This is conducted in order to determine whether or not the prosthetic requires design modifications.

5.1 Introduction

A great deal of research has been focused on evaluating prosthetics as more have become commercially available. Most evaluation techniques, such as those conducted by Miller and Childress, have focussed on measuring the vertical stiffness of prosthetic feet during heel strike (Miller & Childress, 1997). Prince et al. site this technique as having two intrinsic flaws. First, feet with flexible keels should not be evaluated in the same way as prosthetics with rigid keels and articulated ankles. Second, it is difficult to account for energy losses about the keel (Prince et al 1998). Allard et al. (1995) similarly proposed an evaluation based on propulsion and weight transfer at the pushoff stage. These evaluation techniques seem to be effective tools for evaluating the prosthetic as a human aid. However, it is questionable whether these techniques evaluate the similarities between prosthetics and human feet, or if they are simply evaluating the effectiveness of the prosthetic as it will be used by an amputee. Research conducted by P.Quesada (1996) evaluates responsive ankle stiffness of prosthetics by comparing it with human ankle stiffness. In extending the idea of a 'comparative evaluation' proposed by Quesada, a comparative analysis of prosthetic forefoot joint stiffness to the human metatarsophalangeal joint stiffness will be conducted.

In Chapter 3, the stiffness coefficients of the metatarsophalangeal joints of the foot were determined, which will serve in evaluating the prosthetic stiffness. This chapter will determine the stiffness coefficients of the prosthetic foot followed by a brief comparison of the prosthetic stiffness to the human joint stiffness.

5.2 METHODOLOGY

5.2.1 The Prosthetic Used

The prosthetic used in this experiment is the Lifecast model of the Seattle Foot series made by Seattle Limb Systems of Seattle Washington. The Seattle Foot was designed to offer higher levels of function and cosmesis to amputees with a relatively medium activity level. The foot was rated as a male size 9, which results in a 25.1 cm length, and a 9.4 and 8.1 centimeter maximum width and height respectively. The recommended patient weight of the prosthetic is between 125 and 185 lbs (Seattle Limb Systems Catalogue, 1998). This range would accommodate most of the human subjects used in Chapter 3.

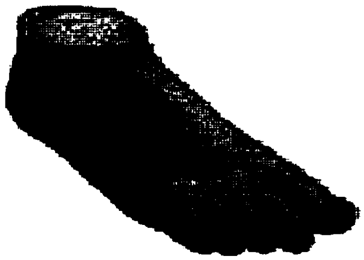

Figure 5.1: Lifecast Model SFH110 -Seattle Limb Systems 1998-

5.2.2 Assumptions

In this experiment, the stiffness coefficients will be determined about the 3 axes defined in Chapter 2. In order to perform this experiment, the following assumptions must be made.

It is noted that the prosthetic, the Seattle Foot, is composed of a homogenous material (urethane) surrounding a delryn keel for stiffness. As shown in Figure 5.3, the keel portion ends approximately 12 mm prior to where the MP joint would be on a human subject. However, the forefoot portion does not have an interior structure and is basically homogeneous with respect to other cross sections of the surrounding region. Since the proposed model implies a rigid forefoot, it must be assumed that the only portion of the foot that will allow rotational motion will be this MP joint area. Therefore, there is no forefoot deformation or rotation within the forefoot body. This assumption is necessary in order to compare the stiffness' with the human foot coefficients. Secondly, the experiment is conducted statically because of our assumption of insignificant damping forces. It is also assumed that the dynamic forces and air capacitance effects of the prosthetic are fairly negligible due to the homogeneity and lack of porosity of the material in the foot which will minimize the air capacitance effects.

5.2.3 Setup

This experiment was performed with the MTS machine setup used in Chapter 4. The MTS was limited to 1 degree of freedom, vertical translation which was used to generate rotation about any given axis of the MP joint center. The MTS was controlled by Testware SX 4.0c and was monitored by the staff at the Calgary Health Sciences complex. Figure 5.2 shows the Seattle foot being held in a testing fixture to correspond with the Z axis. The fixture can be reconfigured to allow rotations about each axis such that the point of contact with the MTS would correspond to 0 degrees forefoot deflection.

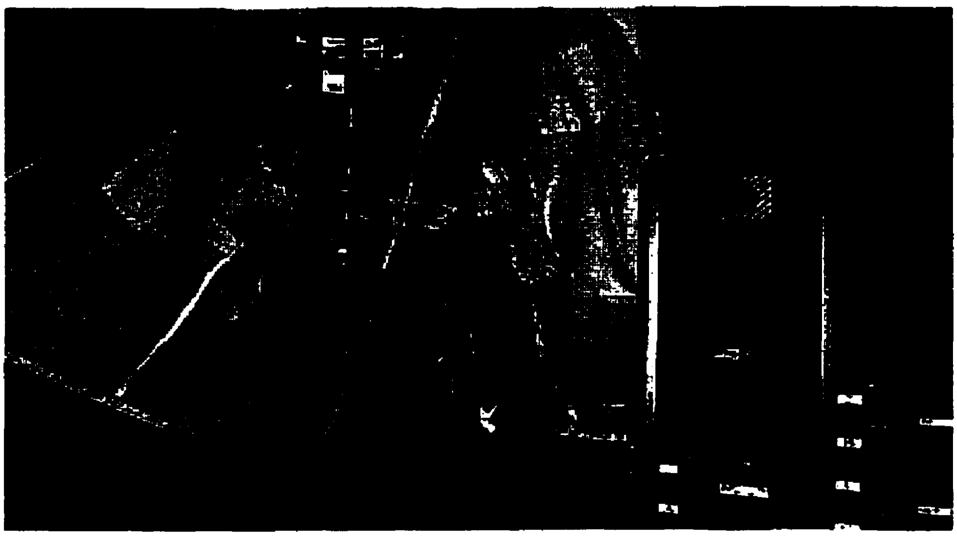

Figure 5.2:Foot Fixture Z-Axis

Additional fixtures for the foot comprised of a U shaped plate which, in the case of the Z axis was tightened to the distal portion of the forefoot as shown in Figure 5.3. The end of this clamp corresponded to Marker 8 in the human tests. This was the most distal portion of the forefoot plane in Chapter 3, and is now the point of application from the MTS to the prosthetic. The distance between the axis and the point of application was ~3.8 cm. After setting the rearfoot to 0 degrees, the protractor was placed on the measuring bars of the forefoot which were bolted to the U-plate.

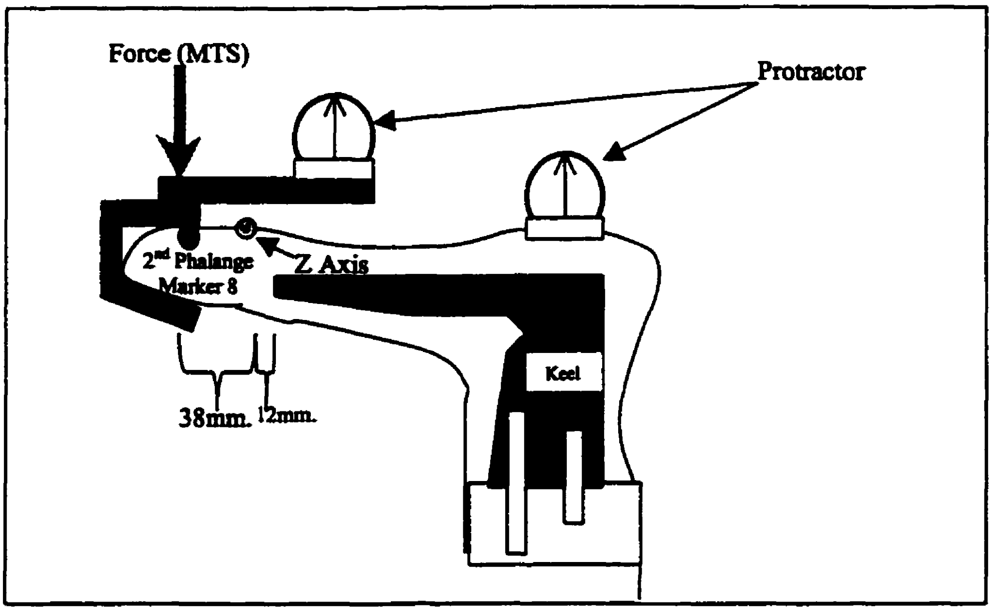

Figure 5.3: Z axis and Fixture Setup

For the Z axis, the force was applied to the underside of the foot such that it would correspond with the movement of the real planar rotation of the human forefoot. This was done so that the measured angle of the prosthetic would correspond with angle of the plane defined by markers 6, 8, and 9, which defined the forefoot in the human model shown previously in Table 3.1. Thus the deflection occurred along the foot from the 2^{nd} toe along the X-axis to 12 mm behind the MP joint resulting in bending area about the Z-Axis approximately 5.0 centimeters wide as shown in Figure 5.4.

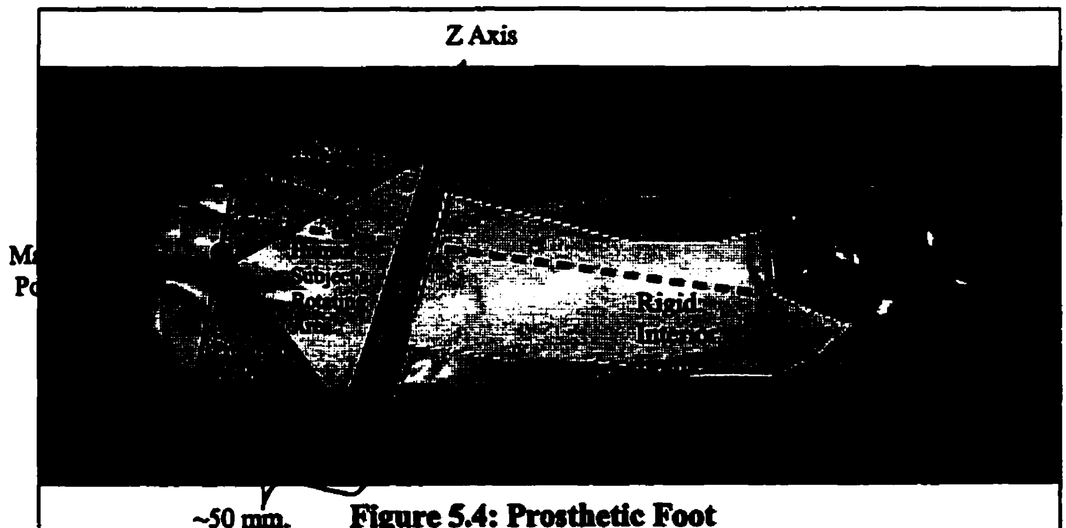

Figure 5.4: Prosthetic Foot

The X axis was tested by constraining the motion about the Y and Z axes and applying a force along a segment from the corresponding 'Marker 8' position to the intersection with the Z axis from MP joint center. Since the rigid member of the foot extends 1.2 cm from the MP joint center, the inversion angle will be a result of the bending along the MTS application segment and this area located posterior to the axis where the frame of the foot ends. The tests about the Y axis are conducted in a similar way, except the force was applied to simulate an adducted motion in a manner corresponding with the X coordinates of Marker 8.

In order to avoid damage to the foot's integrity, fixtures were permanently attached to the foot itself. The tests were done identically to the shoe tests except that there were 5 trials and the actuator moved in a step function, and sampled data for 5 seconds per interval at 2 Hz. The Z axis traveled 2.5 mm per iteration while the X and Y axis were restricted to 1 mm due to the difference in the applied lever arm.

5.2.4 Data Analysis

The data analysis for this experiment was conducted in the same manner as the data in Chapter 4. This is due to the similarity in the testing fixtures used with the MTS.

5.3 Results

In the following section, the stiffness of the foot is presented as a function of changing angle. All data presented is with respect to the segment coordinate system discussed previously, and thus all angles are measured with respect to the rearfoot.

5.3.1 Z Axis

Chapters 3 and 4 have shown that the primary focus for the prosthetic design will be the stiffness about the Z axis due to its functional importance during running and its experimental repeatability shown in Chapter 3. Figure 5.5 shows the stiffness about the Z axis as a function of angle. The stiffness increases dramatically to approximately .38 Nm/deg and then remains relatively constant throughout the remainder of the dorsiflexion range, converging to a value of approximately .42 Nm/deg. The standard deviations of the stiffness may be found in Appendix A. The initial stiffness values which are lower may be a result of the compliance of the material and not of the joint bending. The constant coefficient may be explained as being due to the homogenous material throughout the forefoot section and the tongue insert at the end of the keel of the prosthetic which allows only dorsiflexion of the forefoot.

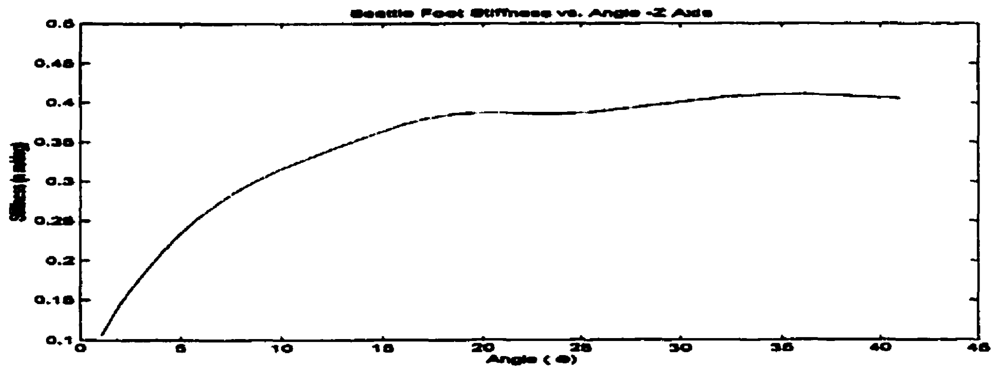

Figure 5.5: Prosthetic Stiffness as a function of Changing Angle (Z Axis)

5.3.2 X and Y Axes

Although the X and Y axes will not be modified in this prosthetic design modification, the stiffness values about these axes are considered because the axial rotations may play larger roles in side stepping and shuffling. The stiffness about the X axis was found to increase more gradually and seems to converge to a value exceeding .6 Nm/deg near 25 degrees. Although our testing range's upper bound was 22 degrees, one may see in Figure 5.6 that the curve does seem to converge. The stiffness may be slightly larger than that about the Z axis due to the larger cross section of material which would naturally affect the angular stiffness. The Y axis demonstrates much different behavior than the X and Z axes. The Y axis demonstrates no convergence to a constant stiffness for the 27 degree range, as shown in Figure 5.7. In fact, the stiffness appears to be increasing linearly at a rate of 0.3 Nm/deg for every 5 degrees flexion. It may be conjectured that the measured stiffness is smaller than the actual stiffness about the axis due to the additional deflection of the local surface deformation at the point of loading.

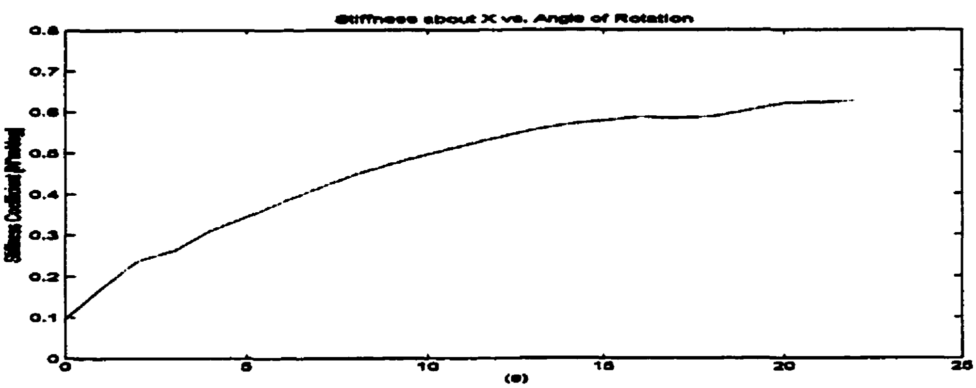

Figure 5.6: Prosthetic Stiffness as a function of Changing Angle -X Axis-

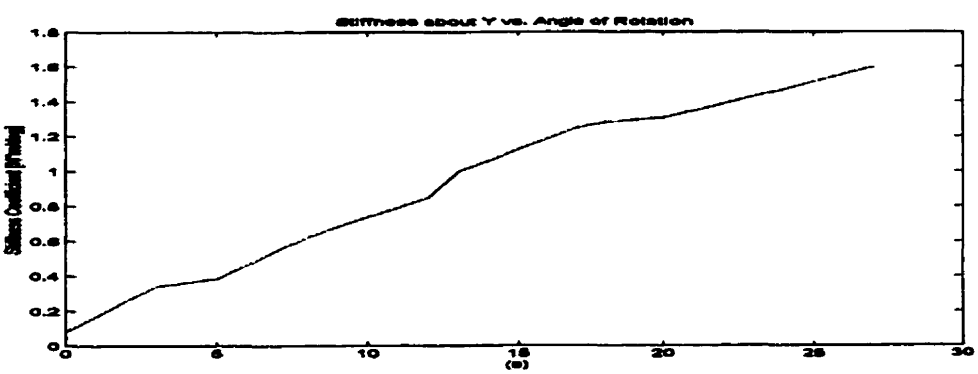

Figure 5.7: Prosthetic Stiffness as a function of Changing Angle -Y Axis-

5.4 Discussion

The objective of this experiment was to determine the stiffness about the Z axis of a Seattle Limb System prosthetic foot. In this section, the stiffness about this axis will be compared to the stiffness of the primary MP axis in the real foot to determine whether or not the prosthetic requires modification.

In Chapter 3, the stiffness of the human MP axis, defined as the Z axis, was determined and found to be nonlinear. It was conjectured that the stiffness about the joints changed with muscular activity, and that during pushoff, the stiffness reaches a brief maximum value within the first 10 degrees of dorsiflexion, and then decreases to a lower nominal value. Section 5.3.1 found that the stiffness of the prosthetic foot converges to a value of approximately 0.42 Nm/deg. Figure 5.8 shows a graph of the human stiffness and the prosthetic stiffness about the Z axis with respect to a change in angle. From this graph one may immediately conclude that the stiffness of the Seattle foot is less than the human stiffness. In addition, due to the linearity of the prosthetic, the Seattle Foot stiffness is relatively constant where the human stiffness is non-linear.

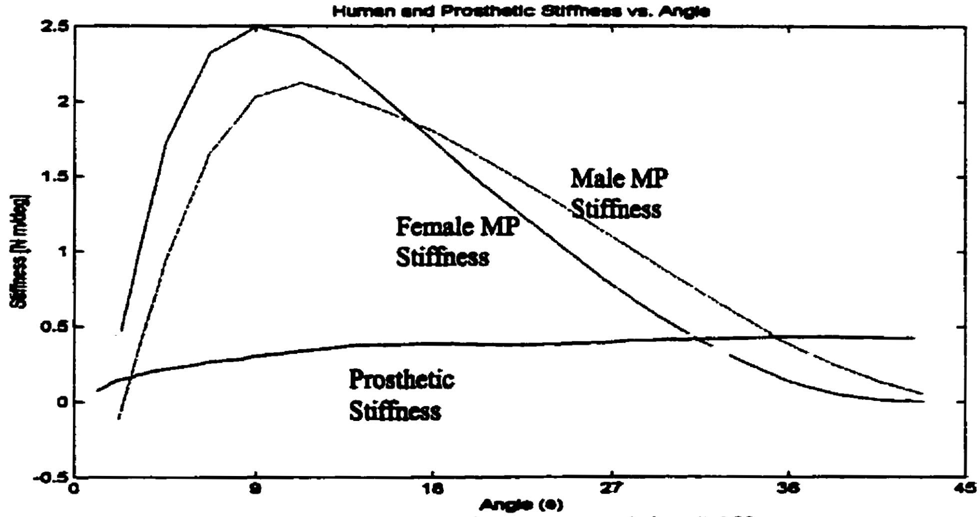

Figure 5.8: Prosthetic / Human Joint Stiffness

Naturally, the stiffness of the human subjects cannot be altered, but a modification to the prosthetic is possible. There are a number of modifications that would be required in order for the prosthetic to replicate the stiffness curves of the human subjects shown. This research will propose one modification that will increase the stiffness to an acceptable value.

A constant stiffness is determined for the human subjects such that it may be compared with the prosthetic stiffness. The stiffness approximation should best represent the characteristics of the human stiffness curve. Since a large portion of the critical events, such as forefoot inversion, occur in the latter half of the push off stage, the region between the maximum stiffness and the stiffness before toe off will be used. The initial portion of the curve will not be used due to the potential errors in the human data due to the sesamoid errors and the small angles used as the denominator in calculating stiffness. Hence, the approximation is obtained by taking the average of the points between the maximum value and the stiffness corresponding to the maximum angles of dorsiflexion. An average of the entire segment between these two points is not necessary due to the relatively constant slope between the maximum stiffness point and the maximum dorsiflexion point. A mean stiffness value of 1.1, with an inter-subject standard deviation of 0.1, was determined from the 6 subjects and was selected as the prosthetic's target stiffness. Therefore, since the stiffness of the prosthetic is between .38 Nm/deg and .42 Nm/deg, the prosthetic is 37% of the human foot stiffness.

Despite the assumptions made previously, it must be acknowledged that the prosthetic does not bend solely along the Z axis defined as the MP joint axis. When a force is applied, the entire forefoot bends similar to how a beam would bend if a force was applied only to one end. One option for increasing the stiffness may be to reinforce a portion of the forefoot to prevent bending along the member. This will be discussed in Chapter 6.

5.5 Summary

In this chapter, the stiffness of the prosthetic was determined to be between .38 and .42 Nm/deg. This was found experimentally using the MTS, fixtures and data analysis tools similar to those used in Chapter 4. It was also found that the stiffness of the prosthetic about the Z axis converged to a value of .42 Nm/deg at 22 degrees but may continue to increase. The upper bounds set for this experiment did not allow further movement. The Y axis exhibited increasing stiffness about the entire range of 0 to 27 degrees with an increase of approximately 3 Nm/deg for every 5 degrees increased. It is conjectured that this may be due to the local surface deformation at the point of loading and the reinforced stiffness of the tongue of the keel. The X and Y axes, however, will not be considered in the first prosthetic modification as explained in Chapter 4.

In comparing the stiffness of the prosthetic to the human stiffness about the Z axis, it was found that while the human stiffness was extremely non linear as a function of angle, the linear characteristics of the elastic material in the prosthetic resulted in a stiffness which was relatively constant. Therefore, it was decided to choose a value for the human stiffness which would approximate the entire curve. This value was chosen to be approximately 1.1 [Nm/deg], found by taking an average of the decreasing portion of the stiffness slopes for both male and female. In limiting the modifications of the prosthetic to one axis, the objective will now be to increase the stiffness of the prosthetic foot to 1.1 Nm/deg in order to approximate the human stiffness curve.

6 MODEL FOR PROSTHETIC MODIFICATION

Before modifying any design, there must be some model on which the modification can be based. In Chapter 5, stiffness about the Z-axis of the human metatarsophalangeal joint was found to be significantly greater than the stiffness of the Z axis, about which dorsiflexion occurs. It was also conjectured that while dorsiflexion, in the human model, occurs about specific axes defined by the metatarsophalangeal joints, the forefoot of the prosthetic bends uniformly with respect to the rearfoot, shown in Figure 6.1. Since there is no joint between the forefoot and rearfoot, and the forefoot of the prosthetic is composed of a homogeneous material, it is assumed that the forefoot bends similar to a homogeneous beam. The objective of this chapter is to determine a possible solution to the problem of the prosthetic's insufficient stiffness due to its distributed bending, and to suggest a possible modification to increase the forefoot stiffness. In addition, this modification will be accompanied by a mathematical justification.

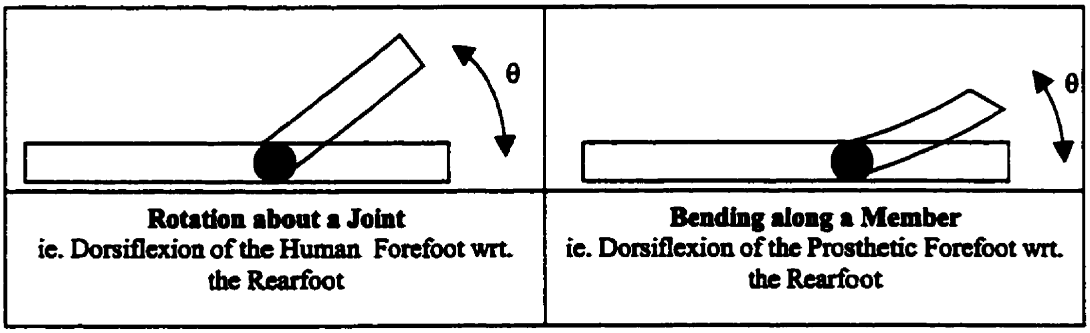

Figure 6.1: Rotation vs. Bending

6.1 Problem and Modification

The Stiffness of the human MP joint was shown to be nonlinear in Chapter 3, but was given a mean constant value so that it may be compared with the linear prosthetic stiffness. Thus in Chapter 5, the human stiffness coefficient was averaged to a value of 1.1 Nm/deg with upper and lower bounds of 1.21 and .99, based on half a standard deviation above and below. These bounds were based on maintaining accuracy within a 0.5 standard deviation of the human subject data. The stiffness of the prosthetic was approximately 0.4 Nm/deg, which means that the stiffness of the prosthetic must be increased by a factor 2.75 ($\pm$ 0.28).

Since the forefoot of the prosthetic bends similar to a beam, it is suggested that by decreasing the area susceptible to bending, an increased stiffness may be obtained, as shown in Figure 6.2. In the first instance the stresses due to bending are distributed along a longer length, while in the other, the stresses are distributed over a smaller length, thus increasing the force required to bend the beam.

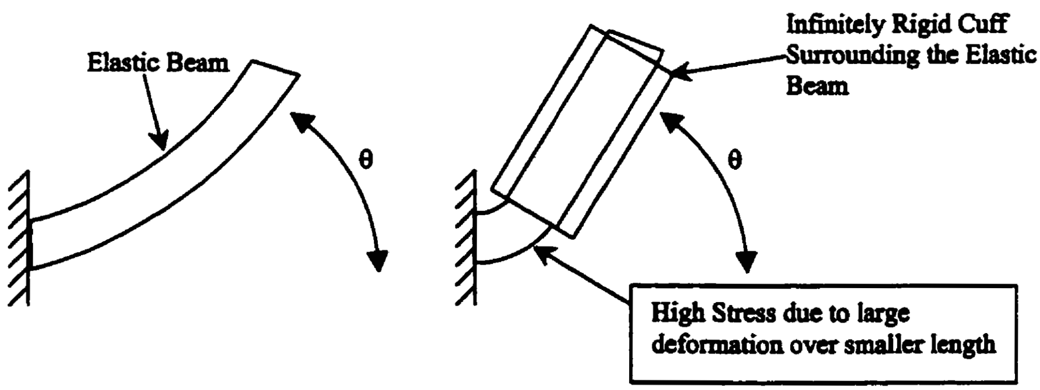

Figure 6.2: Beam Bending and Stiffening

It is recommended that a distal portion of the forefoot be stiffened by making it out of an infinitely stiff material thus reducing the length of the 'beam', and increasing the overall relative stiffness. However, at this time, it may be assumed that a simple plate, rigidly connected to a portion of the forefoot, would simplify the problem of determining the length ratio of bare prosthetic material to the stiffened prosthetic material.

6.2 The Stiffened Length

It is shown in Beer and Johnson (1992) that a beam which is subjected to bending bends into an arc with a radius of curvature, ρ, which is related to the bending moment and the slope angle by Equation 6.1

$$\frac{1}{\rho} = \frac{d\theta}{dx} = \frac{M_b}{EI} \qquad (6.1)$$

Where E=Modulus of Elasticity,
I=Moment of Inertia,
M_b=Moment which varies from section to section as a function of x length.

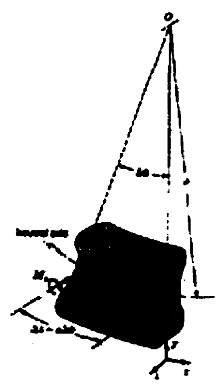

Figure 6.3: Deformation of an Element (Crandall et al. 1978)

Since $M_b = P \cdot x$, integrating 6.1 with respect to dx gives Equations 6.2 and 6.3 of Figures 6.4 and 6.5 respectively, for a slope at the end of a beam.

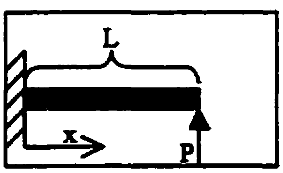

$$\theta = \int_0^L \frac{Px}{EI} dx = \frac{PL^2}{2EI} \qquad (6.2)$$

Figure 6.4: Point Load

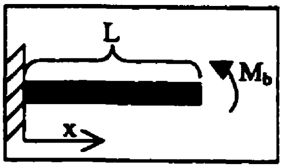

$$\theta = \int_0^L \frac{M_b}{EI} dx = \frac{M_b L}{EI} \qquad (6.3)$$

Figure 6.5: Applied Moment

Equation 6.2 may first be applied to the experimental results obtained in Chapter 5, where a point force is applied to the forefoot, or beam. In applying 6.2 to the experiments of Chapter 5, we obtain Equation 6.4 of Figure 6.6, where P_l is the resultant force of the unmodified foot for a particular angle (θ) and L is the distance from the point force to the distal point of the keel, or frame.

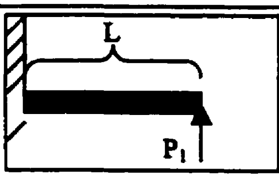

$$\theta = \frac{P_1 L^2}{2EI} \qquad (6.4)$$

Figure 6.6: Point Force Applied to Unmodified Prosthetic foot

However, since the concern of these experiments is stiffness, a correlation to stiffness and force must be made. Since stiffness (K) is defined as the absolute moment divided by the respective absolute angle, in setting θ to a constant value and by increasing the stiffness by a factor n, the Moment (M) and Force (P) increase by a factor n because the length, L, is constant. Thus, an increase in P by a factor n results in a stiffness increase n.

$$K = \frac{M}{\theta} = \frac{PL}{\theta}$$

Therefore, $K \propto P$

In infinitely increasing the stiffness about the distal portion of the forefoot, Equations 6.2 and 6.3 combine to create the following:

$$\theta = \frac{P_2 x_p^{\,2}}{2EI} + \frac{M_2 x_p}{EI} \tag{6.5}$$

Where $L = x_p + x_d$,

P_2= Point force required to obtain angle θ,

and $M_2 = P_2 x_d$.

As shown in Figure 6.7, this equation describes a point force applied to an infinitely stiff beam connected to an elastic beam with a modulus of elasticity E.

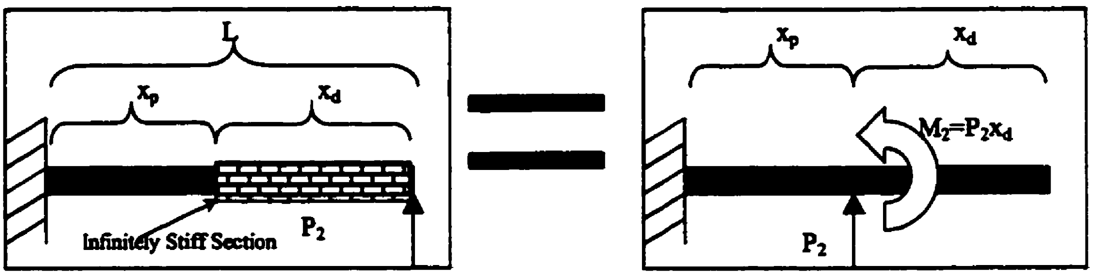

Figure 6.7: Free Body Diagram of Beam with Rigid Attachment

In combining Equations 6.5 and 6.4, we may determine a relationship between stiffness and stiffness length. Equation 6.6 relates the unmodified beam with the modified beam.

$$\frac{P_1 L^2}{2EI} = \frac{P_2 x_p^{\,2}}{2EI} + \frac{M_2 x_p}{EI} \tag{6.6}$$

or by replacing x_d with $L-x_p$, M_2 with P_2x_d and rearranging gives:

$$P_2 x_p^{\,2} - 2P_2 L x_p + P_1 L^2 = 0 \tag{6.6a}$$

Since Equation 6.6a is in the form $Ax_1^2 - Bx_1 + C$, we may solve for x_p using a quadratic equation, which gives:

$$x_p = L\left(1 + \sqrt{1 - \frac{P_1}{P_2}}\right) \tag{6.7a}$$

$$x_p = L\left(1 - \sqrt{1 - \frac{P_1}{P_2}}\right) \tag{6.7b}$$

Since 6.7a gives $x_p \geq L$, it becomes obvious that 6.7b provides a value for x_p, which is the distance between the keel of the foot and the rigid attachment. Thus 6.7b is the desired equation.

The ratio of prosthetic stiffness to human stiffness is between .404 and .331, based on the upper and lower bounds, while the length L is approximately 5cm. ($\pm$ 0.6 cm.). Since the ratio of P_1 and P_2 represent the stiffness ratio between the human stiffness experiments and the prosthetic stiffness experiments, the ratio may now be used as a desired ratio between the desired prosthetic stiffness and the actual prosthetic stiffness. Based on the upper and lower bound ratios for stiffness, the theoretical range of x_p is between .91cm. and 1.1 cm.

It should be pointed out however that the cross sectional area of the foot is not constant and would not be easily described by a function. Thus, any errors between the theoretical x_p length and the actual x_p length may be a result of the false assumption that the moments of inertia for each cross section are the same. The moment of inertia values will actually change as more of the distal portion of the foot becomes infinitely rigid with respect to the rest of the forefoot. If I_1 and I_2 were not equal, it may be shown that:

$$x_p = L\left(1 - \sqrt{1 - \frac{I_2 P_1}{I_1 P_2}}\right) \tag{6.8}$$

Equation 6.8 shows that as the moment of inertia of the foot is increased, the distance between the keel and the rigid distal plates increases. Figure 6.8 shows how the ratio of I_2 and I_1 affects the length of x_1.

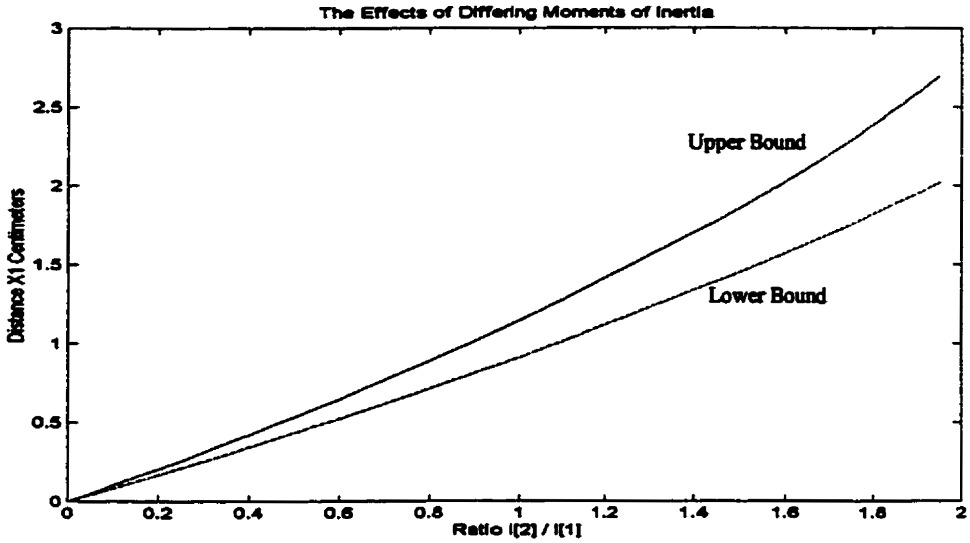

Figure 6.8: The Effects of a Changing Moment of Inertia on x_p

Because the foot tapers towards the toes, the moment of inertia I_2 is greater than or equal to I_1, thus indicating that experimental value of x_p must not be less than the theoretical value of x_p in order for this model to be true.

Since $\quad I_2 \leq I_1$

then,
$$L\left(1-\sqrt{1-\frac{P_1}{P_2}}\right) \leq L\left(1-\sqrt{1-\frac{I_2 P_1}{I_1 P_2}}\right) \tag{6.9}$$

$$x_{p\,(Theoretical)} \leq x_{p\,(Actual)}$$

Having determined the theoretical length that the prosthetic must be stiffened, the following chapter will attempt to prove these findings experimentally.

7 MODIFIED PROSTHETIC EXPERIMENT

7.1 Introduction

Chapter 6 provided the model for the prosthetic modification that is required to reproduce similar stiffness coefficients to that of a human metatarsophalangeal joint during running. The purpose of this chapter is to test out this model in order to see if the desired stiffness is actually obtained.

Many portions of the methodology for this experiment regarding the MTS, the Seattle Foot, and the fixtures are identical to those found in Chapter 5. Thus most of the methodology will be left out of this chapter and may be referred to in Chapter 5. Section 7.1.1 contains the dimensions and construction of the modified parts added to the prosthetic foot to increase its stiffness. Section 7.2 will provide the results of the experiment along with supporting figures. Since the Z axis was chosen as the axis to be modified, only this axis was tested. Section 7.3 will discuss the results and compare them to the target stiffness defined in Chapter 6. Finally, Section 7.4 will summarize the results and evaluate whether the target stiffness was obtained.

7.1.1 The Modification

In this section, a brief description of the modification presented in Figure 6.2 will be provided. Chapter 6 described how to increase the stiffness of a homogeneous, elastic beam. This idea is now applied to the prosthetic foot tested in Chapter 5. It was conjectured that the simplest way to reduce the area for this experiment would be to attach a plate over a portion of the surface of the foot. This should assist in replicating the human target stiffness about the Z axis. However, this may inadvertently increase the stiffness about the X and Y axes. Therefore, in order to reduce the amount of disturbance to the X and Y axes, a series of smaller plates, shown in Figure 7.1, were used instead of a single large plate. The width of the beams will have a direct relationship to the stiffness about the X axis. By similar methods used to calculate the stiffness about the Z axis, the greater the width of the beams, the greater the stiffness will be about the X axis. However, since the focus of the modification is only to affect the Z axis, the effects due to the width of the beams and the effects on the X axis are not discussed here.

The entire length of applied curvature is 5.0 ($\pm$ 0.6) minus the x_p distance of 1.1 ($\pm$ 0.14) centimeters. Therefore the beam lengths were not required to exceed this length. Three beams were chosen in order to maintain the stiffness laterally across the foot. Each beam had 2 holes drilled through each end. A small wire was fed through the holes, which provided the exact distance necessary between each beam. A groove was then filed into the beam as to allow the wire to pass between the beams while not disturbing the foot as shown in Figure 7.1 and 7.2. This attachment was rigidly secured to the bottom of the foot with a thin clamp that secured with a tightening bolt.

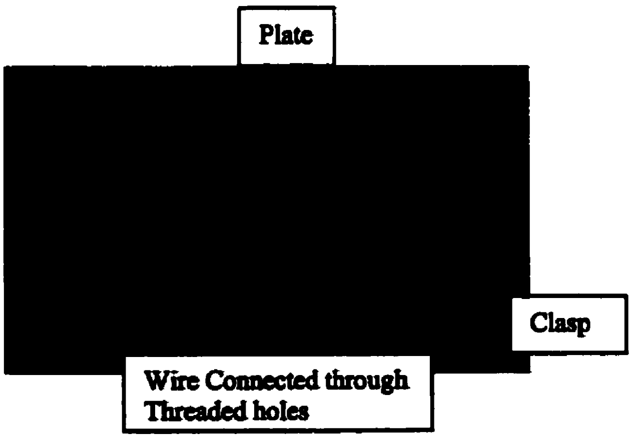

Figure 7.1: Rigidity Attachment

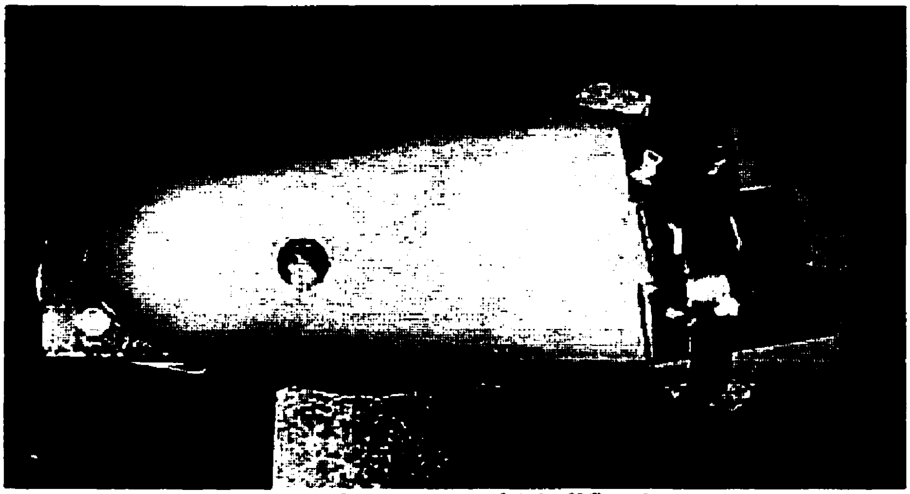

Figure 7.2: Foot and Modification

7.1.2 Methodology

The methodology, and data processing for this experiment was identical to those of Chapter 5. However, in this experiment, 5 trials were taken at $x_p \approx 1.0$ ($\pm$ 0.1) centimeters, and then subjected to 1mm vertical positional increments from the MTS causing rotation about the Z axis.

7.2 Results and Discussion

In modifying the prosthetic, the stiffness about the Z axis has been successfully increased as shown in Figure 7.3. The data between trials were extremely repeatable and thus resulted in extremely small standard deviations as shown in Appendix A. The stiffness coefficient was relatively constant with a mean of approximately 1.03 Nm/deg. The results were relatively predictable based on the trend of the original prosthetic stiffness curves of Figure 5.4 and by the calculations made in Chapter 6. In addition, a preliminary observation shows that the stiffness has increased by approximately 2.5 times the original prosthetic stiffness. These findings prove that the stiffness was increased by reducing the elastic region distal to the Z axis. A brief examination for cracks or strain lines show that the area spanned by x_p was not plastically strained. The fluctuations along the curve are relatively insignificant. The deviation from the mean was less than 4 percent. It is conjectured that these small fluctuations are a result of the slippage between the MTS end effector and the sole surface undergoing the rotational movement.

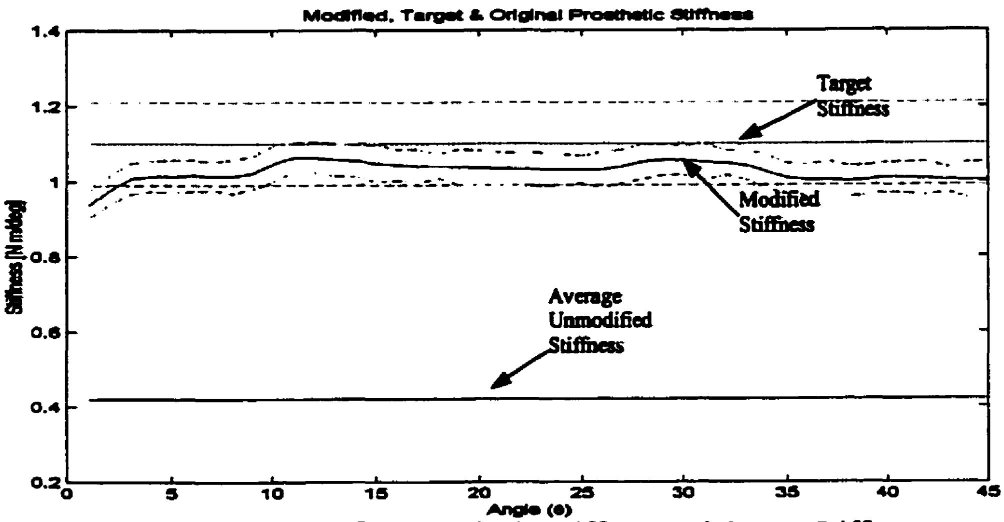

Figure 7.3: Modified Prosthetic Stiffness and Target Stiffness

In Chapter 5 it was found that the stiffness of the prosthetic should be increased by a factor of 2.6 to 2.8. In modifying the Seattle foot, a mean increase of 2.5 to 2.6 times the original stiffness was obtained. The error between the mean value of the modified prosthetic stiffness, and the desired stiffness obtained through human testing is approximately 6 percent as can be seen in Figure 7.4. The difference between these results is relatively insignificant in comparison to the errors present in both the human and the prosthetic testing. In this series of experiments, the errors are mostly attributed to the large error associated with measuring the distal portion of the keel in the prosthetic. A sensitivity analysis shows that an average anterior shift of the axis by 6 mm results in an average decrease of 5% in the total stiffness.

7.3 Conclusion

The goal of the chapter was to modify the prosthetic foot such that the Z axis stiffness would be similar to that of a human foot. This has been achieved by increasing the prosthetic stiffness to a level equal to the average human metatarsophalangeal joint stiffness. Further research should incorporate the X and Y axes into the stiffness model. In addition, different movements that involve inversion or eversion, such as side stepping, may alter the dynamic stiffness coefficients about the axes of the foot and may result in an additional alteration to the prosthetic.

The beams were attached to the exterior of the foot as not to damage the prosthetic but should be flush with the foot as not to affect the shoe fit. This research has determined an approach and modification requirements for a prosthetic foot. However, future research should also focus on adding non homogeneous material to areas of the foot which correspond to additional foot joints such as the inter-phalangeal joints. In achieving this, the foot may be able to display the non-linear stiffness characteristics demonstrated by the human subjects.

8 SUMMARY AND CONCLUSION

This research has produced the following contributions:

- Quantification of stiffness coefficients of the metatarsal joints during running.
- A stiffness comparison between a prosthetic foot and a real foot.
- A design modification to the prosthetic such that its stiffness would better represent a human foot's stiffness.
- Stiffness analysis and testing of the modification.

In Chapter 3, position and force data of 8 subjects were collected using a Kistler force plate, a series of markers, and motion analysis cameras. This data provided the information necessary to calculate the moment about the metatarsophalangeal joint. Stiffness about the joint was then determined by dividing the moment about the axis, by the angle. It was found in each instance that the stiffness of the joint varied non-linearly with the angle of deflection.

In the case of the Z axis, dorsiflexion was found to occur during pushoff, resulting in a maximum stiffness of 2.1 and 2.5 Nm/deg for men and women respectively. The repeatability about this axis is relatively good resulting in a standard deviation of 6 percent of the moment range. The maximum stiffness about the Z axis occurred in the first 15 degrees of dorsiflexion. The data implies that the stiffness is created by the activation of the muscles and ligaments and thus would be directly related to activity levels. Furthermore, it appears that as these muscles provide enough momentum for the push off stage they relax, allowing the phalanges to bend relatively freely about the MP joint, thus reducing the stiffness coefficient while increasing the relative angle.

The angle and moment results obtained from the X and Y axes, for in-eversion, and ad-abduction respectively, were significantly smaller than those found about the Z axis. The standard deviation of the moment data for the Y axis was 12.8 percent and had a mean stiffness value of 0.35 Nm/deg. During the relative inversion of the forefoot an angle of deflection was already present before pushoff commenced. The mean stiffness about the X axis was approximately .65 Nm/deg while the repeatability within the data resulted in a 10 to 13 percent deviation as a function of the range.

The next experiments were designed to determine the stiffness of test shoe samples and the prosthetic foot. The main purpose of testing shoe stiffness was to compare the stiffness values of the shoes with those found in the human foot. It was assumed that if the shoe stiffness was significantly larger than the foot stiffness, then the stiffness of the shoe would dictate the stiffness of the foot-shoe system. In testing 3 shoes it was found that the shoe stiffness varied upon the axis to which the force was applied. For the Z axis, relatively constant values of stiffness were determined, but the magnitude of these values varied depending on the type of shoe used. The stiffness about the Z axis was relatively small ranging from 0.7 to 0.2 Nm/deg. The stiffness about the X and Y axes were found to range from .2 to .7 and .4 to 1.1 Nm/deg respectively. It was determined that the stiffness in inversion of the forefoot may play a more significant role in the forefoot dynamics due to its greater stiffness with respect to the foot stiffness. However, due to the small deflection present, the effects of the shoe on the X axis would likely be negligible for our purpose. The stiffness about the Y axis was found to be stiffer than the stiffness about the X axis. However, one problem was that the angular range was small enough that reducing this range, due to the shoe stiffness, was not necessary. Secondly, the restrictive force on the foot would not be due to the sole of the shoe so much as the material binding the foot to the sole and the sole itself. This resulted in an exclusion of the Y axis from the proposed prosthetic modification.

The stiffness of the prosthetic was then determined by fixing the rearfoot portion, applying forces to the foot, and observing the deflection. The angle was measured about the distal portion of the same forefoot plane defined by the marker allocation in the human experiments. The data showed that the stiffness about the Z axis was 0.42 and constant throughout the entire range. A mean value was taken to represent the human stiffness and was found to be approximately 1.1 Nm/deg. The prosthetic foot did not bend solely along the Z axis, but did in fact bend 1 centimeter behind the axis and bent along the entire length of 4 cm distal to the Z axis. This elastic bending resembles basic beam bending and similar approaches were therefore applied to resolve the problem of insufficient stiffness.

A basic approach was developed to increase the stiffness of the forefoot with respect to the rearfoot about the Z axis. It was proposed that reducing the bendable area in the X-Y plane would increase the stiffness. After determining the length to be stiffened, a series of beam lengths were used to increase the stiffness about the Z axis while not significantly increasing the stiffness about the X axis. The width of the beams used would therefore determine the amount of inversion and eversion of the forefoot. A basic stress analysis determined that the length to be stiffened was 1.01 cm ($\pm$ 0.10 cm.).

In a similar experiment, the stiffness of the modified foot was found to have increased dramatically about the Z axis, reaching a value of 1.03 Nm/deg. These successful results implied that the theory in designing the prosthetic modification was appropriate and thus obtained 'Modified' stiffness values close to desired 'Target' stiffness values.

In conclusion, the results from this thesis have quantified the stiffness coefficients of the forefoot with respect to the rearfoot about 3 axes of motion and compared them with stiffness coefficients obtained using a Seattle Prosthetic Foot. In attempting to mimic human stiffness, the prosthetic was modified by reducing its area to accommodate an increase in the stiffness about the Z axis. It is suggested that future research focus on including a non-linear element to the stiffness about the Z axis, and to further investigate stiffness about the X axis such that the beam width may be modified to accommodate the target values.

References

Abuzzahab F.S., Harris, G.F., Kidder, S.M. Johnson, J.E., Analysis of Foot and Ankle Kinetics During Gait., Proc. IEEE in Medicine and Biology, v17 n2, 1271-1272, Sep, 1995.

Allard P., Trudeau F., Prince F., Dansereau J., Labelle H., Duhaime M., Modelling and Gait Evaluation of Asymmetrical-keel Foot Prosthesis. Medical & Biological Engineering and Computing., v33 n1 p2-7. Jan 1995.

Beer, F. Johnson, R., Mechanics of Materials 2nd Edition. McGrawHill Inc. United States, 1992.

Bejune D., Ouellette J., Zeilinski W., Chen N., Brent P., Norton R.L., Design of a Walking Simulator. Proc ASME. Design Engineering, v71 n2, p463-468. 1994.

Bojsen-Moller, F., Lamoreux, L., Significance of Free Dorsiflexion of the Toes in Walking., Journal of Anatomy, 129 n1, 165-179, 1979.

Carson M., Harrington M., Thompson N., Theologis, T., A four Segment In Vivo Foot Model For Clinical Gait Analysis. Gait & Posture, 73, 1998.

Cavanagh P., The Running Shoe Book. Anderson World Inc., Mountain View Ca. 1980.

Cavanaugh P., Morag E., Boulton A., Young M., Deffner K., Pammer S., Relationship of the Static Foot Structure in Dynamic Foot Function., Journal of Biomechanics v30 n3 p243-250, Mar 1997.

Chan C.W., Rudins A., Foot Biomechanics During Walking and Running., Mayo Clinic Proceedings., 69:448-461, 1994.

Czerniecki, J.M., Gitter A., Munro C., Joint Moment and Muscle Power Output Characteristics of Below Knee Amputees During Running. The Influence of Energy Storing Prosthetic Feet., Journal of Biomechanics v24 n1 p63-75. 1991.

Davies, C., Hindfoot and Forefoot Biomechanics of Children with Clubfoot. C4 Masters thesis. 35-40, 1999.

Davis, R.B., & Deluca P.A., Second Rocker Ankle Joint Stiffness During Gait. Gait and Posture, 3, 79. 1995.

Donatelli R., The Biomechanics of the Foot and Ankle., F.A. Davis Company, Philadelphia, 1990.

Donatelli R., Abnormal Biomechanics of the Foot and Ankle. The Journal of Orthopaedic and Sports Physical Therapy, v9 n1, p11-16, 1987.

Donatelli R., Normal Biomechanics of the Foot and Ankle. The Journal of Orthopaedic and Sports Physical Therapy, v7 n3, p91-95, 1985.

Dozzi P.A., Winter D.A., Ishac, M.G., Relative Role of Ankle and Metatarsal-phalangeal Muscles in Ballet Pointe Work., Journal of Biomechanics v22 n10 p1005, Jun, 1989.

Foulston J., Lord M., West S., Changes in Plantar Surface Shape Induced by Corrective Forefoot Eversion. Clinical Biomechanics, v5 n4 p229-235. Nov 1990.

Francois P., Winter D., Sjonnensen G., Powell C., Wheeldon R., Mechanical Efficiency During Gait of Adults with Transtibial Amputation: Pilot Study Comparing Sach, SEATTLE FOOT, and Golden-Ankle Prosthetics. Journal of Rehabilitation Research and Development, v35 n2, p177-185. 1998.

Fulford, G.E., Veldman, H.J.G, Stewart K., Dynamic Inversion of the Forefoot and Dorsiflexion of the Big Toe Treated by Transfer of Extensor Hallucis Longus. Journal of Bone and Joint Surgery, 21-23. 1989.

Gilchrist L.A. Winter D.A., Multisegment Computer Simulation of normal Human Gait, IEEE trans, Rehabilitation Engineering, v5 n4 p290-299. 1997.

Goldsmith, P, Design of a Robot for Sport Shoe Testing. Proc: 5th International Conference on Control, Automation Robotics and Vision. Singapore. Pp 105-110. Dec, 1998

Gradisar I.M., Noe D.A., Askew M.J., Area Force Relationship in Foot-Floor Contact., American Society of Mechanical Engineers, Bioengineering Division. v29, Jun-July, p489-490. 1995.

Hawes M.R., Nigg B.M. Stefanyshyn D.J. Blue Book Foot and Leg. Adidas America Research and Innovation. Human Performance Laboratory. University of Calgary. 1997.

Hetherington, V.J., Johnson, R.E.J., Albritton, J.S., Necessary Dorsiflexion of the First Metatarsophalangeal Joint During Gait., Journal of Foot Surgery, 218-222. 1990.

Hunter I.W., Kearney R. Dynamics of Human Ankle Stiffness:Variation with Mean Ankle Torque. Journal of Biomechanics v15 n10. p77747-752, 1982.

Hunter I.W., Kearney R. System Identification of Human Joint Dynamics. Abstract: CRC Critical Reviews in Biomedical Engineering, v18 n1, p55-87, 1990.

Joseph, J, Range of Motion of the Great Toe in Men., The Journal of Bone and Joint Surgery, v36B n3, 450-457. Aug. 1954.

Kirsch R., Kearney R.E., Time Varying Identification of Human Ankle Joint Stiffness Dynamics during imposed movement. Proc IEEE Medicine & Biology. v13 pt5 Oct-Nov, p2030-2031. 1991.

Lee, S, Stefanyshyn, D., Nigg B.M. Dynamic characterization of relative forefoot abduction, Submitted to Journal of Biomechanics, 1997.

Lee, S., Relative Forefoot Abduction. Masters thesis, The University of Calgary, Calgary, 1997

Lee, S., Muller, C., Stefanyshyn, D., Nigg, B.M. Relative forefoot abduction and its relationship to foot length in vitro, Clinical Biomechanics v 14 n 3, p193-202, March 1999.

Lemon, D.R., Finite Element model of the Forefoot Interface with Accomodative Footwear Orthoses., American Society of Mechanical Engineers., v31 Nov., p141-142. 1995.

Lord, Marilyn., Spatial Resolution in Plantar Pressure Management., Medical Engineering and Physics., v19 n2 p140-144. Mar 1997.

Mann, R.A., Hagy, J.L., The Function of the Toes in Walking, Jogging and Running., Clinical Orthopaedics and Related Research, n142, 25-29. July-Aug 1979.

Meirovitch L., Methods of Analytical Dynamics. Virginia Polytechnic. McGraw-Hill Book Company. New York. 14-143. 1970.

Miller L.A., Childress D.S., Analysis of a Vertical Compliance Prosthetic Foot, Journal of Rehabilitation Research and Development v34 n1, p52-57. Jan 1997.

Morlock, M. A Generalized Three Dimensional Six Segment Model of the Ankle and the Foot. PhD thesis, The University of Calgary, Calgary, 1989.

Nigg B.M., Biomechanics of Running Shoes. Human Kinetics Publishers Inc. 1986

Nigg B.M., Herzog., Biomechanics of the Musculo-Skeletal System. John Wiley and Sons, England. 1994

Perry J., Boyd L. A., Rao S.S., Mulroy S.J., Prosthetic Weight Acceptance Mechanics in Transtibial Amputees Wearing the Single Axis SEATTLE Lite, and Flex Foot. IEEE Transactions on Rehabilitation Engineering, v5 n4, p283-289. Dec 1997.

Quesada P.M., Pitkin M., Colvin J., Srinivasan, R., Biomediacl Evaluation of a Prototype Foot/Ankle Prosthesis., Proc Southern Biomedical Engineering Conference, p560-562,. Mar29-31, 1996.

Ramon, O., Mizrahi, S., Miltz, J. Merits and Limitations of the Drop and Shock Tests in Evaluating the Dynamic Properties of Plastic Foams. Polymer Engineering and Science., v34 n18. p1406-1410. Sept. 1994

Root, M., Orien W., Weed J., Normal and Abnormal Function of the Foot, Clinical Biomechanics Corporation, Los Angeles, 1977.

Salathe E., Arangio G., A Biomechanical Model of the Foot, Journal of Biomechanics, v19 n12, p989-1001, 1986.

Scott S.H., Winters D.A., Biomechanical Model of the Human Foot: Kinematics and Kinetics During the Stance Phase of Walking., Journal of Biomechanics, v26, n9, 1091-1104. 1993.

Shuizong, H., Fang G., Dynamic Stress Analysis of the Human Foot Metatarsal Bone of Walking at the Flat Ground., Chinese Journal of Biomedical Engineering v16n3, p234-236. 1997.

Sidebottom,B., Advanced Mechanics of Materials 4th Ed. John Wiley and Sons. Canada. 1985.

Stefanyshyn, D.J., Mechanical Joint Energy in Athletics. PhD Thesis. University of Calgary. Calgary, Alberta. 1998.

Stefanyshyn, D.J., Nigg, B.M., Dynamic Angular Stiffness of the Ankle Joint During Running and Sprinting., Journal of Applied Biomechanics, v14 no3 Aug., p292-299, 1998.

Stefanyshyn, D.J., Nigg, B.M., Mechanical Energy Contribution of the Metatarsophalangeal Joint To Running and Sprinting. Journal of Biomechanics, v30 no11/12 Nov/Dec, p1081-1085, 1997.

Stokes I., Hutton W., Stott J., Forces acting on the Metatarsals During Normal Walking, Journal of Anatomy, v129 n3, p579-590, 1979.

Tortora G.J., Grabowski S.R., Principles of Anatomy and Physiology 8th Edition, Harper Collins College Publishers, New York 1996.

Trim D., Multivariable Calculus., Prentice Hall, Ontario. 1993.

-Xia B., Robinson J., A 3D Kinematic Evaluation of Footwear Stability in Lateral Movements, p46-47,1989.

Zhang, L., Drury, C.G., Wooley, S.M. Evaluating the Foot/Floor Interface. Ergonomics v34, n2 p175-192. 1991.

Appendix A:

Standard Deviations

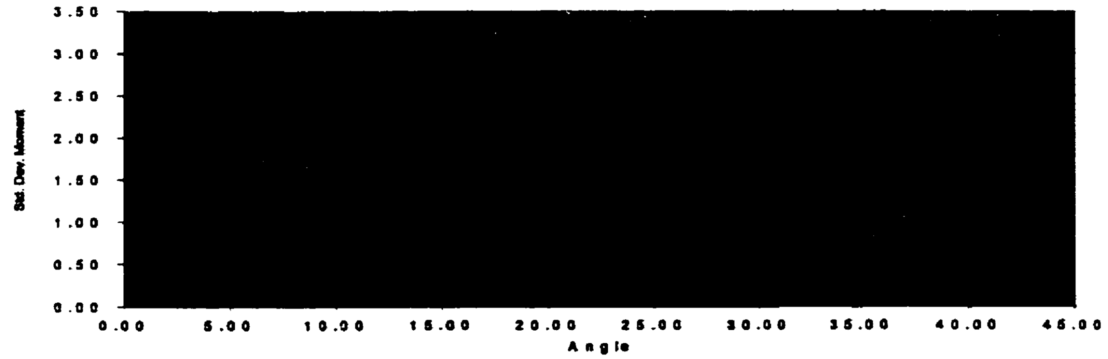

Figure A1: Moment Std. dev vs. Angle (Men, Z Axis)

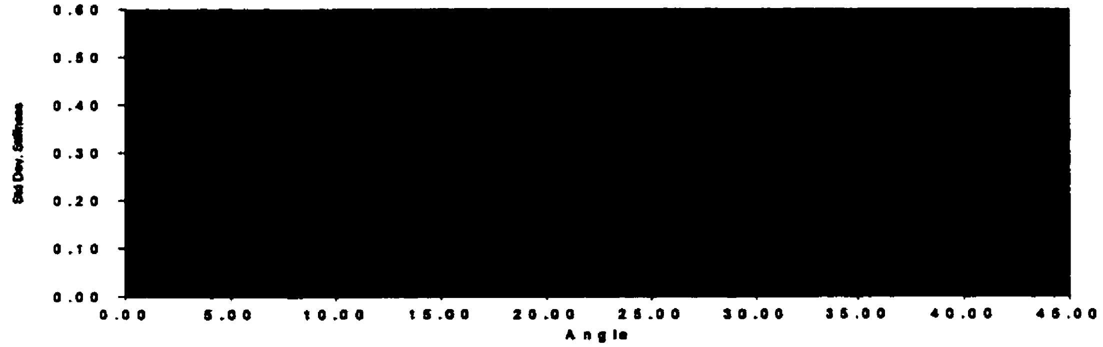

Figure A2: Stiffness Std. dev vs. Angle (Men, Z Axis)

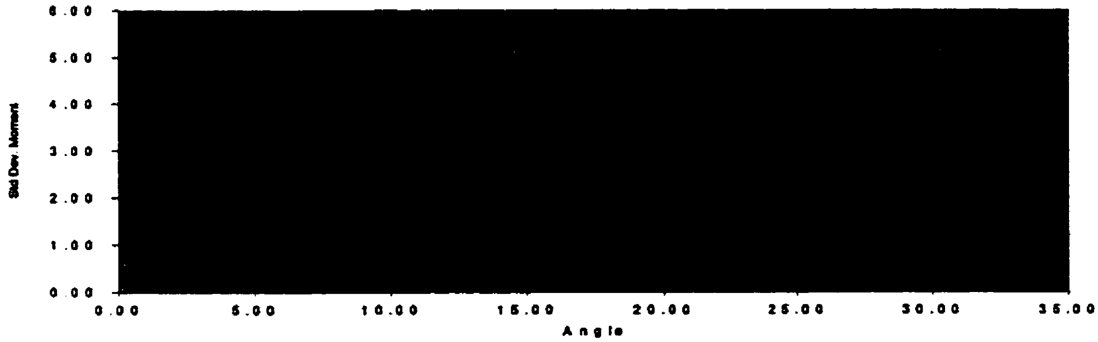

Figure A3: Moment Std. dev vs. Angle (Women, Z Axis)

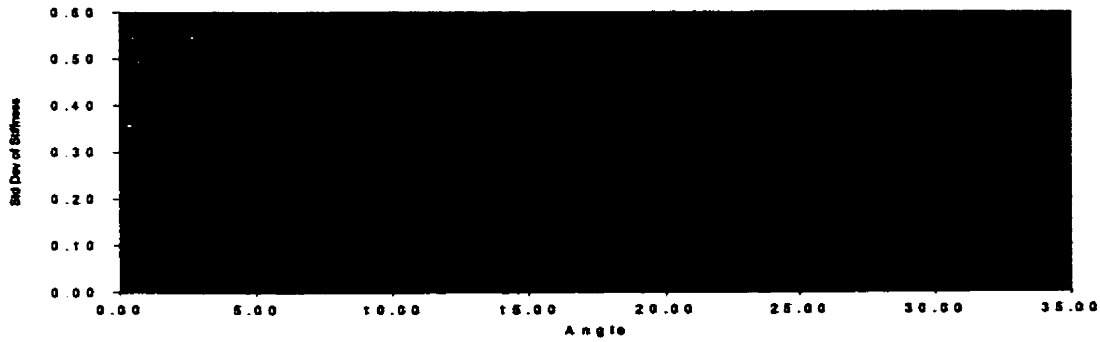

Figure A4: Stiffness Std dev vs. Angle (Women, Z Axis)

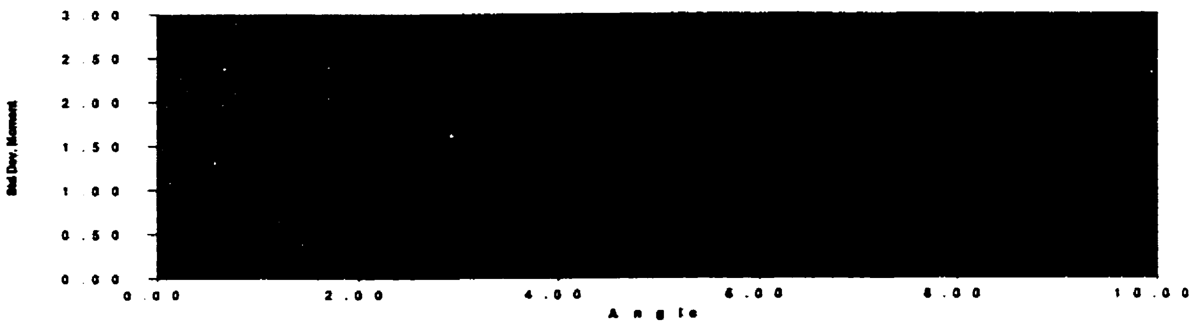

Figure A5: Moment Std. Dev. vs. Angle (Men,Y Axis)

Figure A6: Stiffness Std. Dev. vs. Angle (Men, Y Axis)

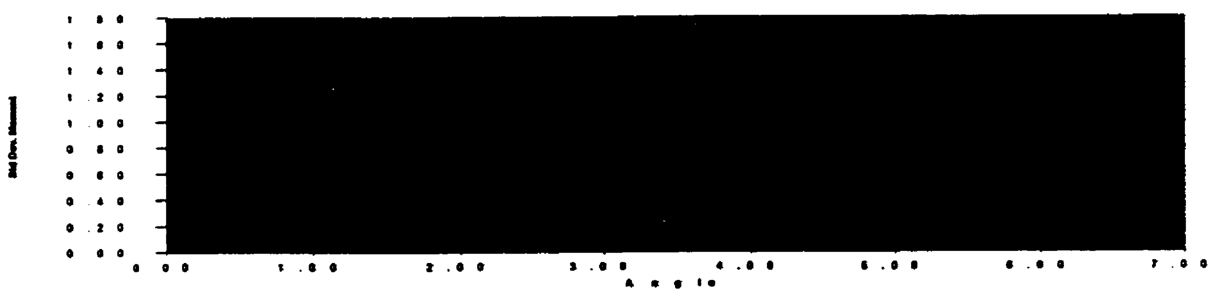

Figure A7:Moment Std. Dev. vs. Angle (Women, Y Axis)

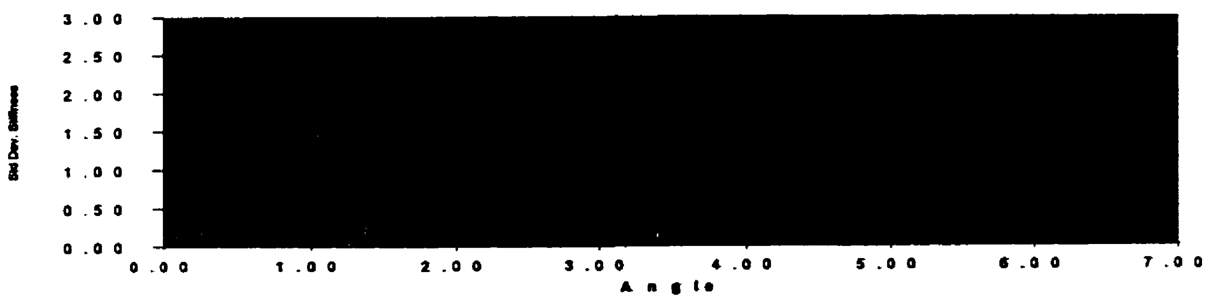

Figure A8:Stiffness Std. Dev. vs. Angle (Women, Y Axis)

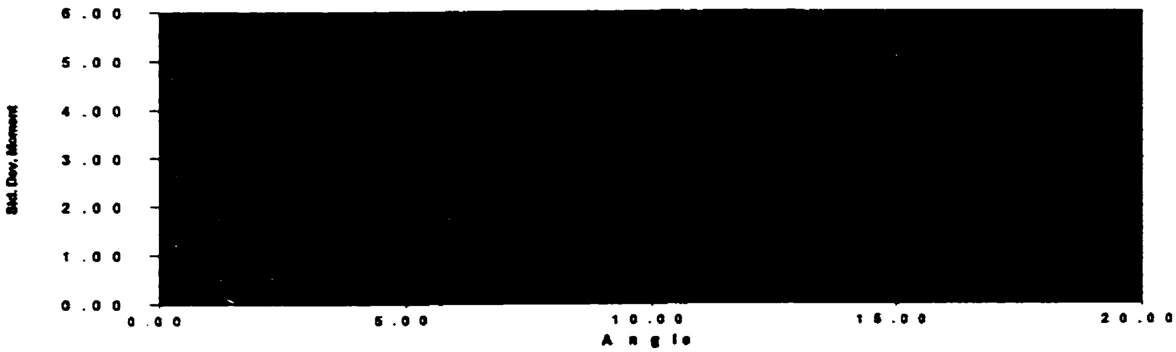

Figure A9:Moment Std Dev. vs. Angle (Men, X Axis)

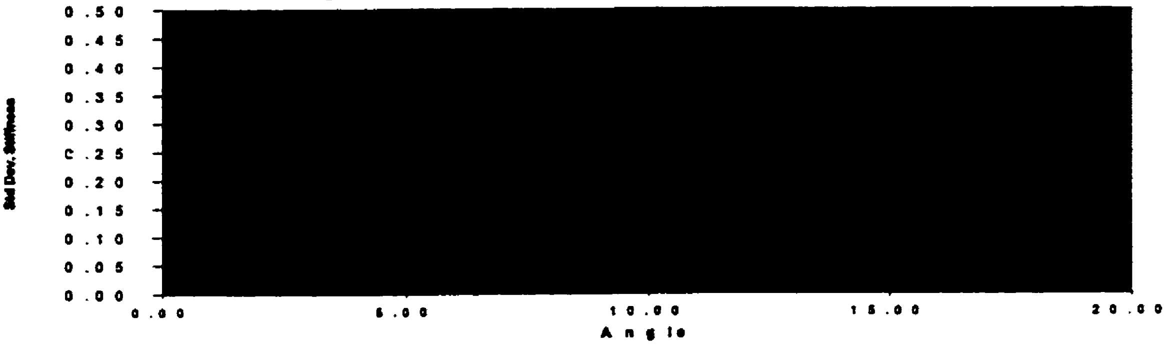

Figure A10: Stiffness Std. Dev. vs. Angle (Men, X Axis)

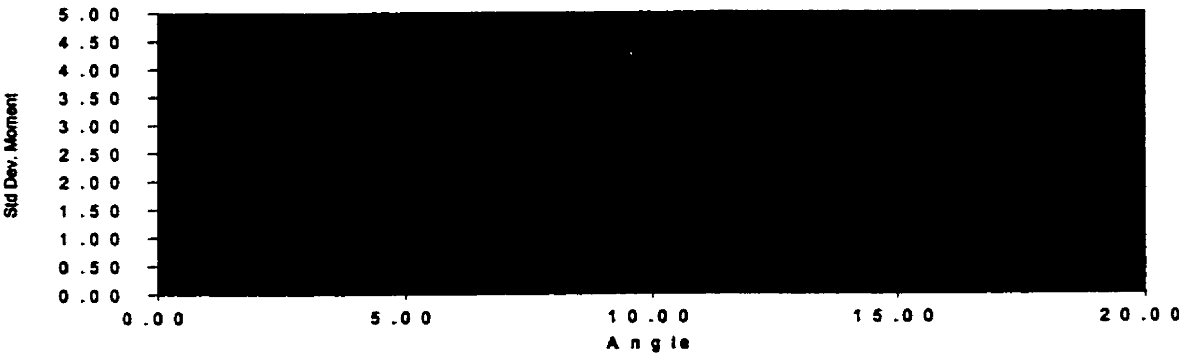

Figure A11: Moment Std. Dev. vs. Angle (Women, X Axis)

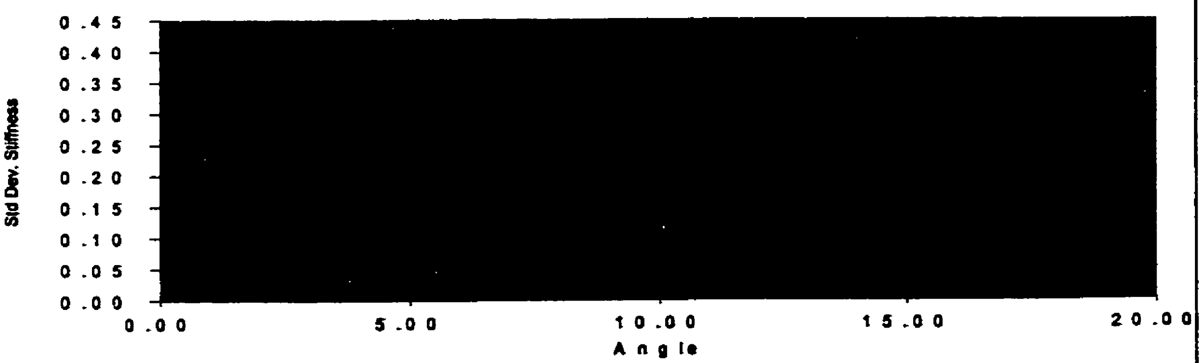

Figure A12: Stiffness Std. Dev. vs. Angle (Women, X Axis)

Standard Deviation -Stiffness-

0.0600(

0.0500(

0.0400(

0.0300(

0.0200(

0.0100(

0.0000(

Std Dev. Stiffness

0.12

0.10

0.08

0.06

0.04

0.02

0.00